

# **International Symposium XeMAT 2015**

Xenon/hyperpolarized noble gases in magnetic resonance

September 13 – 17, 2015 in Dresden, Germany



Impressum

**Technische Universität Dresden**  
**Bioanalytische Chemie**

01062 Dresden

www. <http://www.chm.tu-dresden.de/anc1/>

*Cover Picture*

© Antje Knepper / pixelio.de

*Printed by*

DIEKOPIE25.de GmbH

George-Bähr-Straße 8

01069 Dresden

# Welcome

Dear participants of the international symposium XeMAT 2015,

after the very productive and successful conferences in Sestri Levante, Italy (2000), La Colle-sur-Loup, France (2003), Ottawa, Canada (2006), Ruka-Kuusamo, Finland (2009), and Dublin, Ireland (2012), we – which means: more than 60 registered participants - have now gathered in Dresden in order to discuss the latest developments concerning the use of xenon/ hyperpolarized noble gases in magnetic resonance during the next days. The scientific program of XeMAT 2015 encompasses 29 oral presentations and more than 20 posters. Program details and the abstracts of these contributions can be found in this booklet.

XeMAT 2015 takes place in the new chemistry buildings (Neubau Chemische Institute) which were finished just a few years ago. TU Dresden was founded as an “Institution for Technical Education” in 1828. The first chemistry courses were already offered in 1832. Today, TU Dresden is among the top universities in Germany and Europe. As a modern full-status university with 14 departments it offers a wide academic range making it one of a very few in Germany. TU Dresden is the largest university in Saxony. Since June 2012, TU Dresden is one of eleven German universities that were identified as an “excellence university”.

Let me express my gratitude to the rectorial board and the administration of TU Dresden for providing the facilities and help for the conference organization.

I gratefully acknowledge generous financial support by the *Society of Friends and Promoters of TU Dresden* (“*Gesellschaft von Freunden und Förderern der TU Dresden e.V.*”) and Cortecnet (France).

Finally, it is my hope that you will also enjoy the social program and the beautiful city of Dresden with its numerous sights.

Welcome to Dresden!

Eike Brunner

# Content

1. General Information.....	5
Venue / Locations / Registration / Conference office .....	5
Campus map.....	6
Contact / Internet / Posters / Lunch.....	7
Guided City Tour / Excursion / Conference Dinner.....	8
2. Scientific Program.....	9
Program Schedule.....	9
List of Posters.....	13
3. Abstracts.....	15
Oral Presentations.....	16
Posters.....	74
5. Sponsors.....	118

# 1. General Information

## Venue

The conference will take place in the new buildings of the Department of Chemistry and Food Chemistry (Neubau Chemische Institute, Fachrichtung Chemie und Lebensmittelchemie, Bergstrasse 66, D-01069 Dresden). These buildings are located at the campus of TU Dresden. To reach the campus from the main railway station (“Hauptbahnhof”), take bus no. 66 (direction “Freital/ Mockritz”) and leave it at the station “Mommssenstrasse”. Alternatively, you can also take tram no 3 (direction “Coschütz”) and 8 (direction “Südvorstadt”) and leave it at the station “Nürnberger Platz”. You can also walk from the main railway station (ca. 20-30 minutes walking distance).

For any further questions related to public transportation see also:

<https://www.dvb.de/en-gb/>

## Locations

The lectures will be given in lecture hall no. 2 (room no. 089) in the ground floor of the building. Poster sessions and coffee breaks will take place in the foyer of the same building, next door to the lecture hall.

## Registration/ Conference Office

Foyer “Neubau Chemische Institute”

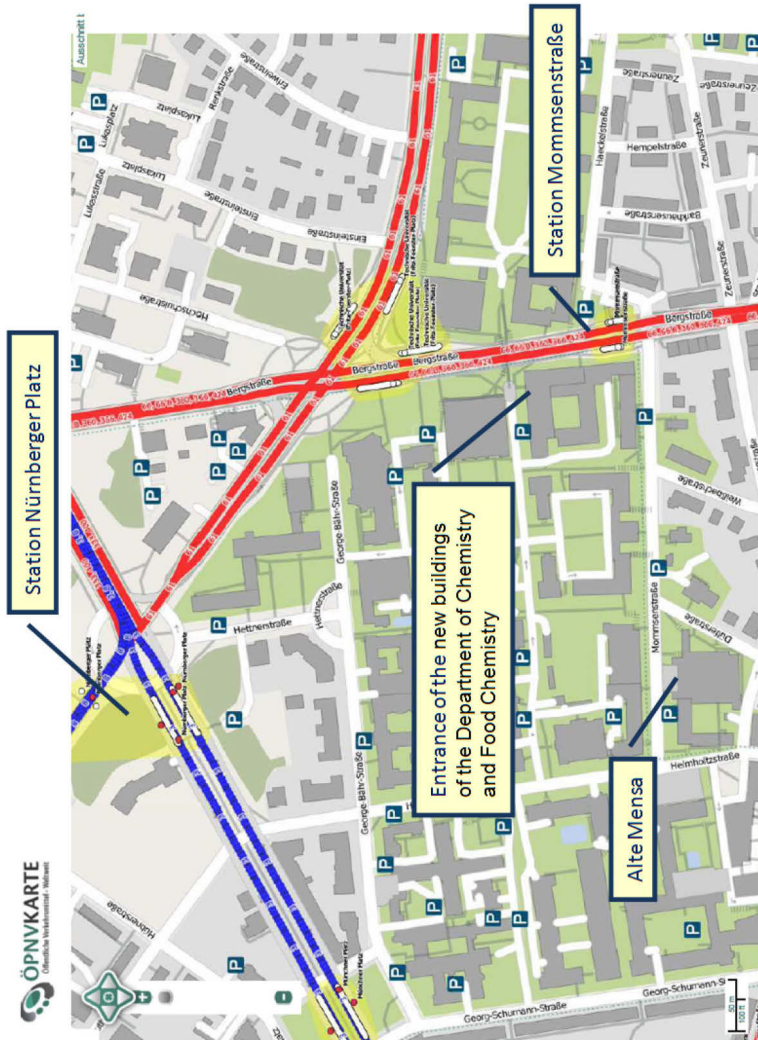
Sunday, 13. 09. 2015                      16:00 – 21:00 h

Monday, 14. 09. 2015                      8:30 – 18:00 h

Tuesday, 15. 09. 2015                      8:30 – 15:30 h

Wednesday, 16. 09. 2015                      8:30 – 13:00 h

Thursday, 17. 09. 2015                      8:30 – 13:00 h



Map data © by Openstreetmap contributors licensed under ODbL 1.0. OPNV map is available under CC-BY-SA licence (© by MeMoMaps).

**Further information:**

<https://navigator.tu-dresden.de/karten/dresden/geb/che/>  
 (Chemistry building in the Campus of TU Dresden)

<https://navigator.tu-dresden.de/etplan/che/00/raum/126600.0460>  
 (Lecture hall in the Chemistry building)

## **Contact**

Office: +49 351 463 32631 or 37152

E-mail: [xemat@mailbox.tu-dresden.de](mailto:xemat@mailbox.tu-dresden.de)

## **Internet access**

We offer a temporary login for the wireless-LAN of the Technische Universität Dresden campus.

The network is called VPN/WEB. If you can't find this network, the wireless-LAN is unfortunately not available at your location. If you are connected to the VPN/WEB network and you open an arbitrary website with your browser, the login window for the wireless-LAN appears. Please enter the user name and password provided. By logging in to this network, you automatically accept the terms and conditions of use as defined by the TU Dresden.

## **Posters**

All posters should be displayed for the entire duration of the conference at the foyer "Neubau Chemische Institute". Posters should be mounted from Sunday 16:00, before first poster session starts. They should be removed at the end of the conference. Presenting authors are requested to be at their poster during the scheduled poster sessions.

## **Lunch**

Lunch vouchers are included for all registered participants and will be handed out during registration. Lunches are served at the building "Alte Mensa" (see campus map on page 6). Students need a student ID.

## **Guided walk through the city center of Dresden**

**Tuesday, September 15, 16:15** The Guided tour starts on "Theaterplatz" in front of the statue of King Johann (in the middle of the square). To reach this site from the TU Dresden campus, please take tram no 8 (direction "Hellerau") and leave it at the station "Theaterplatz".

Afterwards (at 18:00), you have the possibility to attend a devotion with organ recital followed by a guided tour at the "Frauenkirche" ("Church of Our Lady"; free entrance)

## **Excursion to Moritzburg Castle**

**Wednesday, September 16, 14:00** A bus will leave in front of the Hempel-Bau (one of the new buildings of the Department of Chemistry and Food Chemistry) at Mommsenstraße 4 and transfer you to the castle. At 15:00, a guided tour through the castle will start (1h). At 17:00 the bus transfers you back to Dresden.

## **Conference Dinner**

**Wednesday, September 16, 19:00** The Conference dinner will take place at "Sophienkeller im Taschenbergpalais". This restaurant is located opposite the "Zwinger", a famous sight of Dresden (address: Taschenberg 3, 01067 Dresden).



## 2. Scientific program

### Program Schedule

#### Sunday, Sep 13, 2015

16:00	<b>Registration and Poster mounting</b> TU Dresden, Neubau Chemische Institute, Bergstrasse 66, Ground floor, Foyer
19:00	Welcome Mixer

#### Monday, Sept 14, 2015

09:00	Welcome by <b>Prof. Gerhard Rödel</b> – Prorektor für Forschung der TU Dresden
	Opening by <b>Eike Brunner</b> (Dresden)
	<i>Chair: Eike Brunner</i>
09:15	<b>Jacques Fraissard</b> (Paris) $^{129}\text{Xe}$ NMR of Adsorbed Xenon for Materials Characterization
10:05	<b>Stefan Kaskel</b> (Dresden) Nanoporous Materials Characterization: Challenges and Chances
10:40	<b>Erika Weiland</b> (Paris) Contribution of $^{129}\text{Xe}$ NMR spectroscopy to the characterization of texture and transport properties of transition aluminas
11:00	Poster Session one & Coffee
13:00	Lunch
	<i>Chair: Jukka Jokisaari</i>
14:00	<b>Antoine Gédéon</b> (Paris) From Paris to Dresden: Story of our experience with Xenon NMR
14:35	<b>Brian Saam</b> (Salt Lake City) Polarimetry of Hyperpolarized $^{129}\text{Xe}$ Using Rb EPR Frequency Shifts
15:00	<b>Jonathan Birchall</b> (Nottingham) Can Rb/Cs Hybrid Optical Pumping Improve $^{129}\text{Xe}$ Hyperpolarisation?
15:25	<b>Matthias Schnurr</b> (Berlin) Lipid-based nanocarriers for Xe MRI cell labeling

15:45	Coffee & Inf. Poster Session
<i>Chair: Ivan Dmochowski</i>	
16:10	<b>Lars Borchardt</b> (Dresden) Illuminating Adsorption Phenomena in Porous Model Carbons: Structural Characterization Using In Situ High Pressure $^{129}\text{Xe}$ NMR Spectroscopy
16:35	<b>Galina Pavlovskaya</b> (Nottingham) NMR Imaging of Low Pressure, Gas-phase Transport in Packed Beds using Hyperpolarised Xenon-129.
17:00-17:20	<b>Madhwesha Rao</b> (Sheffield) MR imaging and spectroscopy of human brain with hyperpolarized $^{129}\text{Xe}$ at 1.5T

## Tuesday, Sep 15, 2015

<i>Chair: Thomas Meersmann</i>	
09:00	<b>Mitchell Albert</b> (Thunder Bay) Magnetic Resonance Imaging of Hyperpolarized Xenon-129 in the Brain
09:35	<b>Patrick Berthault</b> (Gif sur Yvette) New developments related to fast and multiplexed detection of $^{129}\text{Xe}$ NMR biosensors
10:10	<b>Jukka Jokisaari</b> (Oulu) $^{129}\text{Xe}$ and $^2\text{H}$ NMR study of the properties of liquid crystal dimer CB7CB
10:35	<b>Clancy Slack</b> (Berkeley) Investigation of Differences in Diastereomeric Chemical Shift Response to Metal Ion Chelation by 129-Xenon NMR
11:00	Coffee & Inf. Poster Session
<i>Chair: Heinz Jänsch</i>	
11:35	<b>Agustin Palacios-Laloy</b> (Grenoble) Sensors based on polarized noble gasses
12:10	<b>Guillaume Carret</b> (Gif sur Yvette) 3D-printed system optimizing dissolution of hyperpolarized gaseous species for micro-sized NMR
12:35	<b>Graham Norquay</b> (Sheffield) Pulmonary oxygenation determination using hyperpolarised $^{129}\text{Xe}$ NMR
13:00	Lunch
<i>Chair: Mitchell Albert</i>	
14:00	<b>Leif Schröder</b> (Berlin) Functionalized Xenon for Cellular Labelling in $^{129}\text{Xe}$ MRI: Biosensor Design for High Sensitivity and Specificity

14:35-15:10	<b>Xin Zhou</b> (Wuhan) Multiparametric Evaluation of COPD by Hyperpolarized Xenon ADC and CEST MRI
16:00	Guided walk through the city center of Dresden
18:00	Frauenkirche – devotion, organ recital and guided tour

## Wednesday, Sep 16, 2015

<i>Chair: Jacques Fraissard</i>	
09:00	<b>Neil J Stewart</b> (Sheffield) Methods for hyperpolarised xenon MR imaging of the human lungs and brain
09:35	<b>Ivan Dmochowski</b> (Philadelphia) An Expanded Palette of Xenon Biosensors
10:10	<b>Mikhail G. Shapiro</b> (Pasadena) Genetically Encoded Reporters for HyperCEST MRI
10:45	Poster Session two & Coffee
13:00	Lunch
14:00-18:00	Excursion to Moritzburg Castle
19:00	Conference Dinner

## Thursday, Sep 17, 2015

<i>Chair: Patrick Berthault</i>	
09:00	<b>Maricel Repetto</b> (Mainz) Systematic improvement of $T_1$ times of HP- $^{129}\text{Xe}$ at low fields
09:35	<b>Thomas Meersmann</b> (Nottingham) Relaxation Weighted MRI contrast with Hyperpolarized $^{83}\text{Kr}$ and $^{129}\text{Xe}$ .
10:10	<b>Marie-Anne Springuel-Huet</b> (Paris) A Temporal-Spatial Study of Zeolite Nucleation by Magnetic Resonance of Hyperpolarized Xenon-129 and Transmission Microscopy
10:35	<b>Anu Kantola</b> (Oulu) Can xenon see the paranematic phase of liquid crystal confined to nanocavities?

11:00	Coffee & Inf. Poster Session
<i>Chair: Brian Saam</i>	
11:30	<b>Stephan Appelt</b> (Jülich) EHQE Nuclear Magnetic Resonance Meets Hyperpolarized Gases
12:05	<b>Lorenz Mitschang</b> (Berlin) Kinetics of Cryptophane-Xenon Complex Formation
12:30	<b>Jürgen Senker</b> (Bayreuth) Selective Host-Guest Interactions in Metal-Organic Frameworks
Closing by Eike Brunner	

## List of Posters

**P1** Monitoring of the structural transition in the highly flexible “gate pressure” Metal-Organic Framework  $\text{Ni}_2(2,6\text{-ndc})_2\text{dabco}$  using High-Pressure in situ  $^{129}\text{Xe}$  NMR Spectroscopy

*V. Bon, H. C. Hoffmann, B. Assfour, F. Epperlein, N. Klein, S. Paasch, I. Senkovska, S. Kaskel, G. Seifert, E. Brunner*

**P2** *In-situ* Probing of Catalytic Reaction Dynamics by Means of Xe-129 NMR Spectroscopy

*M. Dvoyashkin, A. Zaheer, J. Zill, J. Matysik, C. Küster, D. Enke, R. Gläser*

**P3**  $^{129}\text{Xe}$  NMR of the Xe in Polyimides with Different Glassy States

*M. Fujita and H. Yoshimizu*

**P4** Characterisation of Acinar Airspace Involvement in Asthma using Inert Gas Washout and Hyperpolarised  $^3\text{Helium}$  Magnetic Resonance

*S. Gonem, S. Hardy, N. Buhl, R. Hartley, M. Soares, R. Kay, R. Costanza, P. Gustafsson, C.E. Brightling, J. Owers-Bradley, S. Siddiqui*

**P5** Probing structure and dynamics of silica based materials by continuous-flow hyperpolarized  $^{129}\text{Xe}$ -NMR

*J. Hollenbach, C. Küster, R. Vialiullin, D. Enke, J. Matysik*

**P6**  $^{129}\text{Xe}$  Hyper-CEST for sensing Supramolecular Complexes

*Jabadurai Jayapaul<sup>1</sup>, Leif Schröder<sup>1</sup>*

**P7 Studying the porosity of MOFs using  $^{129}\text{Xe}$  NMR with hyperpolarized Xe**

*T. W. Kemnitzer, Y. S. Avadhut, E. A. Rössler, J. Senker*

**P8 On Dipolar Interaction – From Line Shape to Spin Diffusion to Double Resonance**

*L. Kraft, A. Potzuweit, A. Schaffner, H.J. Jänsch*

**P9 Impact of Gas Turnover Rate for Improving Hyper-CEST Sensitivity in Xe Biosensor MRI**

*M. Kunth, C. Witte, A. Hennig, L. Schröder*

**P10 Clathrate structures discovered by combination of  $^{129}\text{Xe}$  NMR spectroscopy with crystal structure predictions**

*M. Selent, J. Nyman, M. Ilczyszyn, P. Bygrave, J. Jokisaari, G. M. Day, P. Lantto*

**P11 Hyperpolarized  $^{129}\text{Xe}$  Chemical Exchange Relaxation Transfer**

*C. Lesbats, F. Zamberlan, N.J. Rogers, J.L. Krupa, G.E. Pavlovskaya, N.R. Thomas, H.M. Faas, T. Meersmann*

**P12 A doubly responsive probe for the detection of Cys4-tagged proteins**

*E. Mari, N. Kotera, E. Dubost, G. Milanole, E. Doris, E. Gravel, N. Arhel, T. Brotin, J.-P. Dutasta, J. Cochrane, C. Boutin, E. Léonce, P. Berthault, B. Rousseau*

**P13 In situ  $^{129}\text{Xe}$  and  $^{13}\text{C}$  NMR spectroscopic investigations of the porosity switching in  $\text{Zn}_2(\text{BME-bdc})_x(\text{DB-bdc})_2\text{-xdabco}$**

*J. Pallmann, H. C. Hoffmann, V. Bon, E. Eisbein, I. Schwedler, I. Senkovska, R. Fischer, G. Seifert, S. Kaskel, E. Brunner*

**P14 Absolute measurement of the Xe polarization**

*M. Repetto, P. Blümler, W. Heil, S. Karpuk and S. Zimmer*

**P15 Ultra-narrow Line Diode Laser Systems for Optical Pumping of K, Rb, Cs, and Ar Gases**

*A. Ryasnyanskiy, L. Chase, T. Wood, V. Smirnov, O. Mokhun, A. Glebov, L. Glebov*

**P16 In situ variable pressure  $^{129}\text{Xe}$  NMR of zirconium-based metal organic frameworks**

*J. Schaber, I. Senkovska, S. Kaskel, E. Brunner*

**P17 Using in situ Raman and NMR Spectroscopies to Map the Dependences of Spin-Exchange Optical Pumping and Energy Transport on Xenon Density**

*J.G. Skinner, H. Newton, J. Birchall, N. Whiting, M. J. Barlow, B. M. Goodson*

**P18** FEM Analysis of Diffusive Exchange of Hyperpolarised  $^{129}\text{Xe}$  in the Human Lungs using Realistic Histology-Based Geometries

*N. J. Stewart, J. Parra-Robles, J. M. Wild*

**P19** Investigation of Xenon-Based Sensors in Oriented Environments

*A. Truxal, C. Slack, C. Vassiliou, M. Gomes, P. Dao, K. Jeong, D. Wemmer, A. Pines*

**P20** MRI of metabolically labeled glycans using Hyper-CEST xenon biosensors in a live-cell bioreactor.

*C. Witte, L. Schröder*

**P21** Novel high-volume, standard pressure  $^{129}\text{Xe}$  SEOP polarizer with spectrally width narrowing laser system

*A. Wojna-Pelczar, T. Pałasz*

**P22** Fine Structure of Glassy State of Polymers through the  $^{129}\text{Xe}$  NMR Chemical Shift and Xe Sorption Properties

*H. Yoshimizu*

### **3. Abstracts**

Oral presentations and Posters

## Talk1

# **$^{129}\text{Xe}$ NMR of Adsorbed Xenon for Materials Characterization**

**J. Fraissard**

University Pierre and Marie Curie, ESPCI-LPEM, 10 rue Vauquelin, 75005 Paris, France

The  $^{129}\text{Xe}$  NMR technique was initially introduced in 1980 [1] for the characterization of the free space of zeolites. The adsorbed  $^{129}\text{Xe}$  detected by NMR is an excellent probe to determine microporous solid properties difficult to detect by classical physico-chemical techniques. Indeed the very large and extremely polarisable electron cloud of xenon makes this atom particularly sensitive to its immediate environment. Small variations in the physical interactions with the latter cause marked perturbations of the electron cloud which are transmitted directly to the xenon nucleus and greatly affect the NMR chemical shift.

Since 1991, this technique has taken a new turn with the advent of hyperpolarized xenon [2] in the characterization of materials. The use of HP-Xe increases the sensitivity for the detection of xenon by several orders of magnitude. The range of its applications becomes wider each day.  $^{129}\text{Xe}$  NMR is applied now for the characterization of a lot of solids: micro- and mesoporous silico-aluminates, clays, liquid crystals, metal-organic framework compounds (mainly their elasticity), porous carbons, solid polymers, metal catalysts and even ancient pictures. It can also be used to determine the type of diffusion of molecules in microporous structures.

### **References:**

- [1] T. Ito, J. Fraissard, *Proc of the 5th Int Zeolite Conf*, ed. Rees L.V., Heyden and son, London, GB, (1980) 510-515.
- [2] D. Raftery, H. Long, T. Meersmann, P. J. Grandinetti, L. Reven, A. Pines, *Phys Rev Lett*, **66(5)** (1991) 584-587.



**Notes:**

## Talk 2

# Nanoporous Materials Characterization: Challenges and Chances

S. Kaskel

TU Dresden, Bergstr. 66, Dresden, Germany

Porous materials have gained significant importance in energy storage and transformation systems. Innovative gas and heat storage systems as well as battery technologies profit from custom made pore structures of only few nanometers in diameter. Recent advances in the field of porous materials have pushed the limits towards higher surface areas and record values beyond 7000 m<sup>2</sup>/g were achieved. However, topology, interconnectivity and polarity of the inner surface are equally important.

Metal-Organic Frameworks (MOFs) have emerged as a new class of porous materials with ultrahigh porosity, well defined structure and porosity. They are promising materials for gas storage (natural gas) and separation processes. However, the assessment of pore size distributions and polarity characterization remains a challenge. An exceptional feature of some MOFs is *flexibility in the solid state* [1]. These gas-triggered crystal-to-crystal transformations (also called *gating* crystals) show a unique porosity switch from a closed pore (cp) to an open pore (op) form, a cooperative step-wise transition, with a high potential for applications in switchable catalysts, filters, threshold sensors, or stimulus induced drug delivery. However, so far only a limited number of such compounds are known, and more important, the underlying principles responsible for such a high degree of flexibility are not understood, which is essential to explore the applicability of such networks in separation and catalysis further [2]. The development of in situ monitoring methods is an essential task to develop this field further. Xe NMR is a valuable tool to monitor such transitions in situ and gain a better understanding of pore-probe interactions [3].

For battery applications, nanoporous carbons with specific surface areas are in the focus of research. Especially hierarchical porous carbons with micropores (< 2 nm) and larger pore channels (10-100 nm) are key components for electrochemical storage. They show high power densities in supercapacitors and high energy densities in next generation batteries such as the lithium sulfur battery [4]. Xe

NMR is an ideal tool to understand adsorption mechanisms and connectivity in hierarchical porous carbons [5].

The presentation will give insights into modern materials requirements and fundamental questions associated with nanoporous materials design and applications.

**References:**

- [1] A. Schneemann, V. Bon, I. Schwedler, I. Senkowska, S. Kaskel and R. A. Fischer, *Chem. Soc. Rev.*, **43** (2014) 6062-6096.
- [2] N. Klein, C. Herzog, M. Sabo, I. Senkowska, J. Getzschmann, S. Paasch, M. R. Lohe, E. Brunner and S. Kaskel, *Physical Chemistry Chemical Physics*, **12** (2010) 11778-11784.
- [3] H. C. Hoffmann, B. Assfour, F. Epperlein, N. Klein, S. Paasch, I. Senkowska, S. Kaskel, G. Seifert and E. Brunner, *J. Am. Chem. Soc.*, **133** (2011) 8681-8690.
- [4] C. Hoffmann, S. Thieme, J. Brueckner, M. Oschatz, T. Biemelt, G. Mondin, H. Althues, S. Kaskel, *ACS Nano*, **8** (2014) 12130-12140.
- [5] M. Oschatz, H. C. Hoffmann, J. Pallmann, J. Schaber, L. Borchardt, W. Nickel, I. Senkowska, S. Rico-Frances, J. Silvestre-Albero, S. Kaskel, E. Brunner, *Chem. Mater.* **26** (2014) 3280-3288.

### Talk 3

## Contribution of $^{129}\text{Xe}$ NMR spectroscopy to the characterization of texture and transport properties of transition aluminas

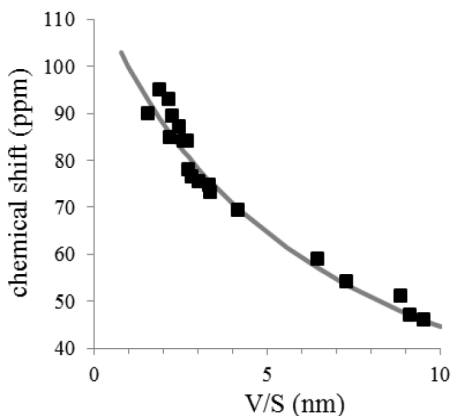
E. Weiland,<sup>1,2</sup> M.-A. Springuel-Huet,<sup>1</sup> A. Nossov,<sup>1</sup> F. Guenneau,<sup>1</sup> A.-A. Quoineaud,<sup>2</sup> A. Gédéon<sup>1</sup>

<sup>1</sup>Sorbonne Universités, UPMC Univ Paris 06, UMR 7574, Laboratoire de Chimie de la Matière Condensée de Paris, F-75005, Paris, France

<sup>2</sup>IFP Energies nouvelles-Etablissement de Lyon, F-69360, Solaize, France

The characterization of textural and transport properties of hydrotreatment catalyst supports (transition aluminas) is decisive for IFP Energies nouvelles to better understand the impregnation processes of metal salt solutions into the mesoporosity of alumina.

The chemical nature of the alumina surface greatly depends on the activation temperature and has a marked influence on the chemical shift of adsorbed xenon. To overcome this difficulty in order to correlate the chemical shift to the pore size, experimental conditions have been optimized: low activation temperature (573 K) and a sufficiently high Xe pressure (minimum 600 torrs). In these conditions, the Xe chemical shift does not depend much on the presence of strong adsorption sites on the alumina surface. It was therefore possible to establish a correlation between the measured chemical shift and the surface-to-volume (V/S) ratio of aluminas (see Figure below).



As used previously for zeolites [1] and then for silicas [2] a simple exchange model between an adsorbed and a gas phase was applied. By fitting the experimental results with the theoretical chemical shift expression [2] values of  $\delta_a$  (characterizing the Xe-surface interaction) and  $K_{ads}$  (adsorption constant) were determined. Whereas  $\delta_a$  is similar for aluminas (117 ppm) and silicas (118 ppm), the difference observed for  $K_{ads}$  ( $2.8 \times 10^{16}$  and  $1.3 \times 10^{16} \text{ Pa}^{-1} \text{ m}^{-2}$ , respectively) was explained by the pore surface which may present different rugosity for amorphous silicas and crystalline aluminas. To study the pore connectivity of bimodal aluminas, 2D EXSY experiments performed at 263, 293 and 313 K allow us to quantify exchange rate between different types of pores or between the pores and the gas phase. Self-diffusion coefficients of xenon and n-hexane have been measured by pulse field gradients NMR and give valuable information on the tortuosity of the porous network.

## References

- [1] J. Fraissard, T. Ito, M. Springuel-Huet, *Stud Surf Sci Catal*, **28** (1986) 393-400.
- [2] V. Terskikh, I. Moudrakovski, *Langmuir*, **18** (2002) 5653-56.

## Talk 4

### From Paris to Dresden: Story of our experience with Xenon NMR

Erika Weiland, Marie-Anne Springuel-Huet, Andrei Nossov, Flavien Guenneau,

A. Gédéon\*

LCMCP, Sorbonne Universités, UPMC Univ Paris 06, CNRS, Collège de France, Laboratoire de Chimie de la Matière Condensée de Paris, 11 place Marcelin Berthelot, 75005 Paris, France.

We all share that xenon is one of the most useful nuclei to probe the pore properties and local structure of porous materials. We were also all surprised by the great enhancement of the  $^{129}\text{Xe}$  NMR sensitivity achieved by optical pumping which has extended the application of the technique to materials with low surface area or long relaxation times.

In this lecture, a series of various experiments performed over the last 3 decades, using thermal and hyperpolarized xenon will be presented: Applications on zeolites, mesostructured materials, silica films, encapsulated molecules in nanomaterials [1], alumina industrial catalysts [2], etc. Furthermore, I will illustrate the structural changes occurring with the flexible frameworks of porous hybrid inorganic–organic compounds [3,4] by hyperpolarized  $^{129}\text{Xe}$  NMR

#### References:

- [1] F. Guenneau, K. Panesar, A. Nossov, M.-A. Springuel-Huet, T. Azaïs, F. Babonneau, C. Tourné-Péteilh, J.-M. Devoisselle and A. Gédéon Probing the mobility of ibuprofen confined in MCM-41 materials using MAS-PFG NMR and hyperpolarised- $^{129}\text{Xe}$  NMR spectroscopy, *Phys. Chem. Chem. Phys.*, **15**, 18805-18808 (2013)
- [2] Exploring the Complex Porosity of Transition Aluminas by  $^{129}\text{Xe}$  NMR Spectroscopy, E. Weiland, M.-A. Springuel-Huet, A. Nossov, F. Guenneau, A.-A. Quoineaud, and A. Gédéon *J. Phys. Chem* DOI: 10.1021/acs.jpcc.5b03211 (2015)
- [3] M.-A. Springuel-Huet, A. Nossov, Z. Adem, F. Guenneau, C. Volkringer, T. Loiseau, G. Férey and A. Gédéon  $^{129}\text{Xe}$  NMR Study of the Framework Flexibility of the Porous Hybrid MIL-53(Al) *J. Am. Chem. Soc.*, **132** 11599–11607 (2010)
- [4] M.-A. Springuel-Huet, A. Nossov, F. Guenneau, A. Gedeon, Flexibility of ZIF-8 materials studied using Xe- $^{129}\text{Xe}$  NMR, *Chemical Communications* **49** 7403-7405 (2013)

**Notes:**

## Talk 5

# Polarimetry of Hyperpolarized $^{129}\text{Xe}$ Using Rb EPR Frequency Shifts

Z.L. Ma<sup>1</sup> and B. Saam<sup>2</sup>

<sup>1</sup> Department of Chemistry, Washington University in St Louis. St. Louis, Missouri, USA

<sup>2</sup> Department of Physics and Astronomy, University of Utah, Salt Lake City, Utah, USA

We report on our latest efforts to develop *in-situ* Rb EPR frequency-shift polarimetry for  $^{129}\text{Xe}$ . The work started several years ago with a measurement [1], under normal spin-exchange optical pumping (SEOP) conditions, of the dimensionless enhancement factor  $\kappa_0$  for Rb- $^{129}\text{Xe}$ , a parameter which characterizes the collisional Fermi-contact interaction and allows the EPR shift to be calibrated to an absolute  $^{129}\text{Xe}$  polarization. Motivations for this work include the introduction of a reliable polarimetry standard for apparatus designed to produce large volumes of hyperpolarized xenon, and the potential to improve quality and precision of measurements of  $^{129}\text{Xe}$  spin-exchange rates and efficiencies. SEOP was performed using a 17-watt frequency narrowed laser-diode array operating at the D<sub>1</sub> transition wavelength (795 nm). A 70 mW transverse probe laser, circularly polarized and detuned from the 780 nm (D<sub>2</sub>) transition in Rb, was intensity-modulated at the at the 19.9 MHz hyperfine transition frequency by weakly-driven  $^{87}\text{Rb}$  atoms in an applied field of 2.81 mT. The derivative of the modulation signal was used as feedback to stabilize the voltage-controlled oscillator generating the weak rf field. The main applied DC magnetic field is unshielded but current-stabilized with an external FET and comparator. The measured EPR frequency shift thus corresponds to a real-time measurement of the mean hyperfine field sensed by the  $^{87}\text{Rb}$  atoms during Fermi-contact collisions as the  $^{129}\text{Xe}$  atoms become polarized. Data from measurements done on a 5-cm dia. spherical cell containing natural Rb and 0.2 amgt Xe (enriched to 90%  $^{129}\text{Xe}$ ) are shown in Fig. 1(a). Fig. 1(b) shows the corresponding  $^{87}\text{Rb}$  ( $F=2$ ) EPR hyperfine spectrum. The relative intensities of these peaks can be used [2] to determine independently the electron polarization  $P_{\text{Rb}} = \langle S_z \rangle / S$  of the Rb atom ensemble that generated the curve in Fig. 1(a).



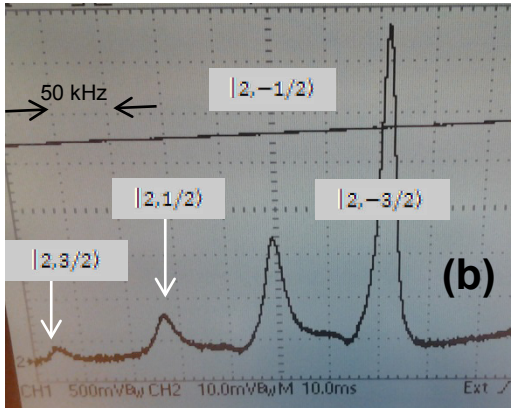
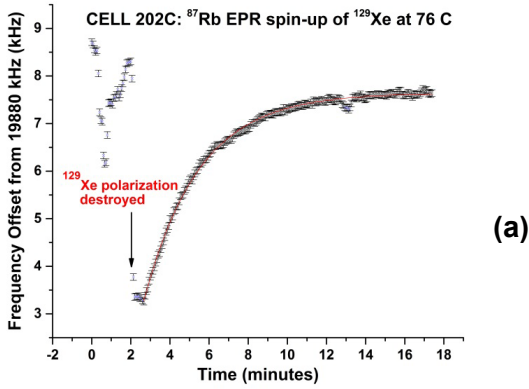


**Figure 1:** (a) Rising transient of  $^{129}\text{Xe}$  nuclear polarization (subsequent to being destroyed by a rapid series of 33.3 kHz NMR pulses) produced by SEOP with Rb, as detected in by modulation of the Faraday rotation signal of the transition

$|F, m_{F_i}\rangle \rightarrow |F, m_{F_f}\rangle = |2, -2\rangle \rightarrow |2, -1\rangle$  in  $^{87}\text{Rb}$ , corresponding to the tallest peak in the  $^{87}\text{Rb}$  hyperfine spectrum, shown in (b). The peaks in (b) are labeled according to the short-hand notation:

$|F, m_{F_i}\rangle \rightarrow |F, m_{F_f}\rangle = |F, (m_{F_i} + m_{F_f})/2\rangle$ . The Rb polarization, as determined from the peak intensities in (b), is 60%. The final  $^{129}\text{Xe}$  polarization, based on Ref. [1] and the observed 4.35 kHz shift, is 8.7%.

#### References:

- [1] Z.L. Ma, E.G. Sorte, and B. Saam, *Phys. Rev. Lett.* **106** (2011) 193005.
- [2] A. Ben-Amar Baranga, S. Appelt, *et al.*, *Phys. Rev. A* **58** (1998) 2282-2294.

## Talk 6

### Can Rb/Cs Hybrid Optical Pumping Improve $^{129}\text{Xe}$ Hyperpolarisation?

**Jonathan Birchall<sup>1</sup>, Hayley Chung<sup>2</sup>, Jason Skinner<sup>1</sup>, Nicholas Whiting<sup>3</sup>, Brogan M. Gust<sup>4</sup>, Kaili Ranta<sup>4</sup>, Michael J. Barlow<sup>1</sup>, & Boyd M. Goodson<sup>4</sup>**

<sup>1</sup>Sir Peter Mansfield Imaging Centre, University of Nottingham, Nottingham, NG7 2RD, UK

<sup>2</sup>Time Medical Limited, Science Park West Avenue, Hong Kong Science Park, Shatin, N.T., HK

<sup>3</sup>The University of Texas MD Anderson Cancer Center, Houston, TX 77030, USA

<sup>4</sup>Department of Chemistry and Biochemistry, Southern Illinois University, Carbondale, IL 62901, USA

Hyperpolarised (HP)  $^{129}\text{Xe}$  has numerous applications in both medical and scientific fields. These include MR imaging and spectroscopy, investigating host-guest interactions of molecules, as well as probing surfaces and porous media. Typically, HP gases are produced via spin-exchange optical pumping (SEOP), where angular momentum is transferred from circularly polarised, resonant photons to the electronic spins of an alkali metal vapour, and is subsequently imparted onto the  $^{129}\text{Xe}$  nuclei. This creates a HP gas with nuclear spin polarisation many orders of magnitude greater than at thermal equilibrium, thus enabling its many applications.

Rubidium is the chosen alkali metal vapour for most SEOP experiments due to the availability of high power frequency-narrowed lasers at the D<sub>1</sub> wavelength, large spin-exchange cross-section and high spin-exchange efficiency with  $^{129}\text{Xe}$ . Jau *et al.* [1] showed that the binary spin-exchange rate coefficient for Cs- $^{129}\text{Xe}$  is ~1.6 times greater than for Rb- $^{129}\text{Xe}$ ; furthermore Gibbs and Hull [2] presented that the nuclear spin-exchange cross-section is ~1.2 times greater for Rb<sup>87</sup>-Cs<sup>133</sup> than Rb<sup>87</sup>-Rb<sup>87</sup>. A K/Rb hybrid approach for  $^3\text{He}$  SEOP has also shown desirable enhancement using a standard 795 nm Rb laser [3]. This investigation follows recent work by Whiting *et al.* [4], where caesium (which has increased vapour pressure relative to Rb) pumping resulted in a ~two-fold improvement in  $^{129}\text{Xe}$  nuclear spin polarisation compared to Rb- $^{129}\text{Xe}$ . The work presented here

investigates a Rb/Cs hybrid approach aiming to examine the polarisation obtainable from Rb/Cs SEOP.

We present results examining the Rb/Cs hybrid using NMR spectroscopy, as well as from the temperature of the nitrogen buffer gas which is added into the optical pumping cell at various cell positions. N<sub>2</sub> is present to pressure broaden the alkali metal transition, allowing increased absorption of laser light and also to quench excited states of the alkali metal by collisional de-excitation, preventing emission of unpolarised light. N<sub>2</sub> temperature can be measured by *in-situ* Raman spectroscopy, first shown by Walter *et al.* [5] and later refined and demonstrated by our group with higher powered lasers in binary Xe/N<sub>2</sub> mixtures. This showed elevated cell temperatures not measured by the cell surface thermocouple which is commonly used to measure the oven temperature.

This hybrid technique may lead to increased <sup>129</sup>Xe polarisation obtained from Cs/Xe SEOP whilst making use of more developed (and more efficient) Rb D<sub>1</sub> laser technology. It may also be able to utilise high powered Rb D<sub>1</sub> frequency-narrowed lasers present on many hyperpolarisers within the community. As such, this may be a simple and cheap addition with an increased gain to the system.

#### References:

- [1] Y.-Y. Jau, N. N. Kuzma, W. Happer, *Phys. Rev. A* **66** (2002) 052710
- [2] H. Gibbs, R. Hull, *Phys. Rev.* **153**(1) (1967) 132
- [3] E. Babcock, *et al.*, *Phys. Rev. Lett.* **91**(12) (2003) 123003-1
- [4] N. Whiting, *et al.*, *Phys. Rev. A* **83** (2011) 053428
- [5] D. K. Walter, W. M. Griffith, W. Happer, *Phys. Rev. Lett.* **86**, (2001) 3264

## Talk 7

### Lipid-based nanocarriers for Xe MRI cell labeling

**Matthias Schnurr, Karl Sydow, Honor May Rose, Margitta Dathe,  
and Leif Schröder**

Leibniz-Institut für Molekulare Pharmakologie, Robert-Rössle-Strasse 10,  
13125 Berlin, Germany

Chemical Exchange Saturation Transfer combined with hyperpolarized xenon (Hyper-CEST) [1] is a highly sensitive technique to detect contrast agents such as cryptophane-A (CrA) in the nano-molar range. Recently, the first Xe-MR images of live cells using CrA cages as a label were obtained [2]. For future in vivo experiments, high local cage loads, cytotoxicity, and unspecific cellular uptake of CrA are remaining challenges. Here, we investigate the biocompatible and selective delivery of CrA to Human Brain Microvascular Endothelial Cells (HBMECs) via electrostatic targeting through arginine-rich peptides and compare the labeling efficiency of liposomal and micellar nanocarrier systems. The Hyper-CEST MRI results are supported by fluorescence methods.

Both carrier systems consisted of phospholipids with peptide labeled headgroups. The micellar system contained covalently bound CrA whereas in the liposomal system CrA was post-inserted through hydrophobic interaction. Both systems were stable in size for several weeks and a significant reduction in cytotoxicity compared to naked CrA enabled by the lipid environment was found. NMR and MRI experiments of  $1 \times 10^6$  cells/mL were performed at a field strength of 9.4 T. Xe hyperpolarization (25 %) was produced using a custom-designed continuous flow Xe polarizer [3]. Figure 1 compares the Hyper-CEST spectra of two cell samples after incubation. Using the micellar system, the unfavored resonance of  $\text{Xe@CrA}_{\text{aqueous}}$  vanished, which must be due to the covalent binding of CrA in the lipid phase. In Xe MRI experiments less contrast between the HBMECs and an aortic control cell line was obtained after cellular uptake of the micellar system compared to the liposomal system, yet it was more efficient in terms of concentration (25-fold) and incubation time (4-fold).

Using liposomal based nanocarriers to deliver CrA to cells provides multiple advantages: i) hydrophobicity and ii) toxicity issues of CrA are both bypassed; iii) such systems are well studied drug carriers which can be modified for different targeting purposes; iv) they enable very efficient CEST amplification and are MRI detectable at nano-molar concentrations. Hence, those easy to modify building block approaches pave the way for future applications with highly sensitive Hyper-CEST MRI in diagnostics and theranostics.

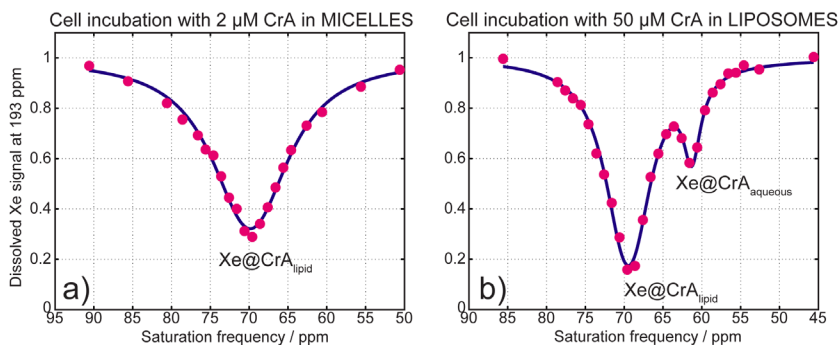


**Figure 1:**  $^{129}\text{Xe}$  Hyper-CEST spectra of  $1 \times 10^6$  cells/mL incubated with micelles (a) and liposomes (b) carrying 2 and 50  $\mu\text{M}$  CrA, respectively, at 37  $^\circ\text{C}$ . In a), the unwanted resonance of  $\text{Xe@CrA}_{\text{aqueous}}$  was not detected. Parameters for a):  $B_1 = 20 \mu\text{T}$ ,  $t_{\text{sat}} = 10 \text{ s}$ ,  $t_{\text{incubation}} = 1 \text{ h}$ . Parameters for b):  $B_1 = 10 \mu\text{T}$ ,  $t_{\text{sat}} = 8 \text{ s}$ ,  $t_{\text{incubation}} = 4 \text{ h}$ .

## REFERENCES:

- [1] Schröder *et al. Science* **314** (2006);
- [2] Klippel *et al. Angew Chem* **126** (2013); Rose *et al. PNAS* **111** (2014); Shapiro *et al. Nat Chem* **6** (2014);
- [3] Witte *et al. J Chem Phys* **140** (2014)

## Talk 8

# illuminating Adsorption Phenomena in Porous Model Carbons: Structural Characterization Using In Situ High Pressure $^{129}\text{Xe}$ NMR Spectroscopy

L. Borchardt,<sup>1</sup> M. Oschatz,<sup>1</sup> J. Silvestre-Albero,<sup>2</sup> S. Kaskel,<sup>1</sup> E. Brunner<sup>3</sup>

<sup>1</sup> Department of Chemistry and Food Chemistry, Institute of Inorganic Chemistry, TU Dresden, Germany

<sup>2</sup> Laboratorio de Materiales Avanzados, Departamento de Química Inorgánica-Instituto Universitario de Materiales, Universidad de Alicante, Spain

<sup>3</sup> Department of Chemistry and Food Chemistry, Bioanalytical Chemistry, TU Dresden, Germany

Porous and nanostructured carbons are key-components in various energy- and environmentally relevant applications such as catalysis, gas adsorption/gas separation, and electrochemistry. In many cases, the performance of these materials is strongly correlated to their pore structure (i.e. the size, geometry, connectivity, and surface chemistry of the cavities).

The classical volumetric physisorption of gases (i.e. nitrogen at 77 K, argon at 87 K or carbon dioxide at 273/298 K) will likely remain the most important methods for the textural characterization of porous materials surfaces on the nanoscale. However, alternative methods are very useful to get deeper understanding of the pore structure and its interaction with adsorbate molecules.

Here we present In situ high pressure  $^{129}\text{Xe}$  NMR spectroscopy in combination with volumetric adsorption measurements for the textural characterization of different carbon model materials with well-defined porosity ranging from the micro- (<2nm) to the mesopore level (2-50 nm). [1] It displays a sensitive technique to measure the micropore diameter and allows gaining insight into the connectivity of pore systems and the adsorption state of gases within the confined space of a pore (Fig.1).

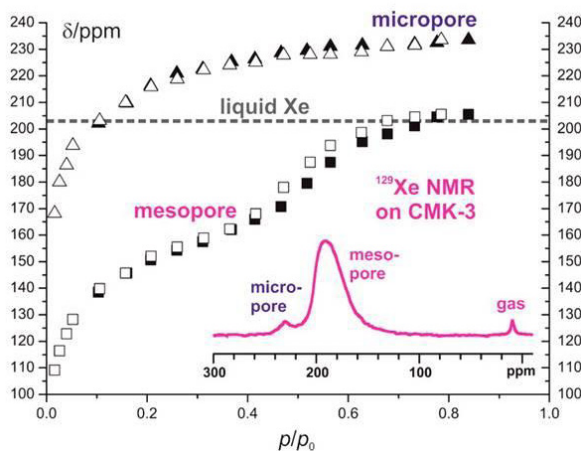


**Fig.1**  $^{129}\text{Xe}$  NMR chemical shift of Xe adsorbed at 237 K within the mesopores and micropores of model carbon materials as a function of relative pressure.

#### References:

- [1] Martin Oschatz, Herbert C. Hoffmann, Julia Pallmann, Jana Schaber, Lars Borchardt, Winfried Nickel, Irena Senkowska, Soledad Rico-Francés, Joaquín Silvestre-Albero, Stefan Kaskel, Eike Brunner; *Chem. Mater.* **26** (2014) 3280-3288.

## Talk 9

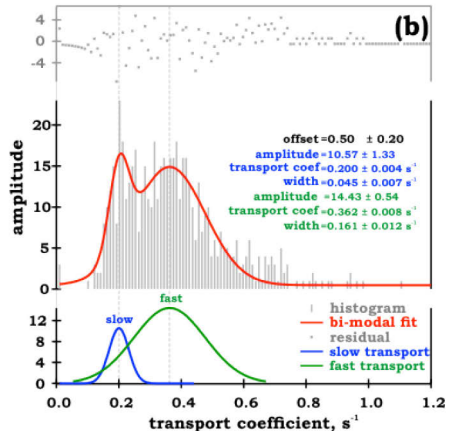
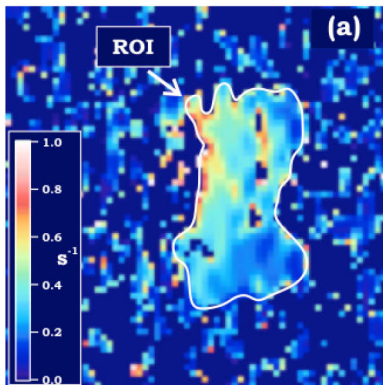
# NMR Imaging of Low Pressure, Gas-phase Transport in Packed Beds using Hyperpolarised Xenon-129.

Galina Pavlovskaya<sup>1</sup>, Thomas Meersmann<sup>1</sup>, Sean P. Rigby<sup>2</sup>

<sup>1</sup> Sir Peter Mansfield Imaging Centre, School of Medicine, University of Nottingham, University Park, Nottingham, NG7 2RD, U.K.

<sup>2</sup> Department of Chemical and Environmental Engineering, University of Nottingham, University Park, Nottingham NG7 2RD, U.K.

Gas-phase MRI has been used to investigate heterogeneity in mass transport in a packed bed of commercial, alumina, catalyst supports. Hyperpolarized <sup>129</sup>Xe MRI enables study of low-density, gas-phase mass-transport, such that diffusion can be studied in the Knudsen regime, and not just the molecular regime, which is the limitation with other techniques. Knudsen-regime diffusion is common in many industrial, catalytic processes. Significantly larger spatial variability in mass transport rates across the packed bed was found compared to techniques using only molecular diffusion. It has thus been found that these heterogeneities arise over length-scales much larger than ~100 microns [1].





To our knowledge this is the first quantitative study of transient diffusion for microscopic porous systems using xenon chemical shift to selectively image gas within the pores. This will enable the gas transport heterogeneity across the pellets and the bed to be observed and measured directly and non-invasively. The approach is particularly sensitive to intra-batch variability in commercial pellets. In particular, the method permits the study of pellet heterogeneity on diffusion in the Knudsen regime at relatively low fluid density.

**References:**

- [1] Galina Pavlovskaya, Navin Gopinathan, Joseph Six, Thomas Meersmann, Sean P. Rigby: *AIChE J*, under review.

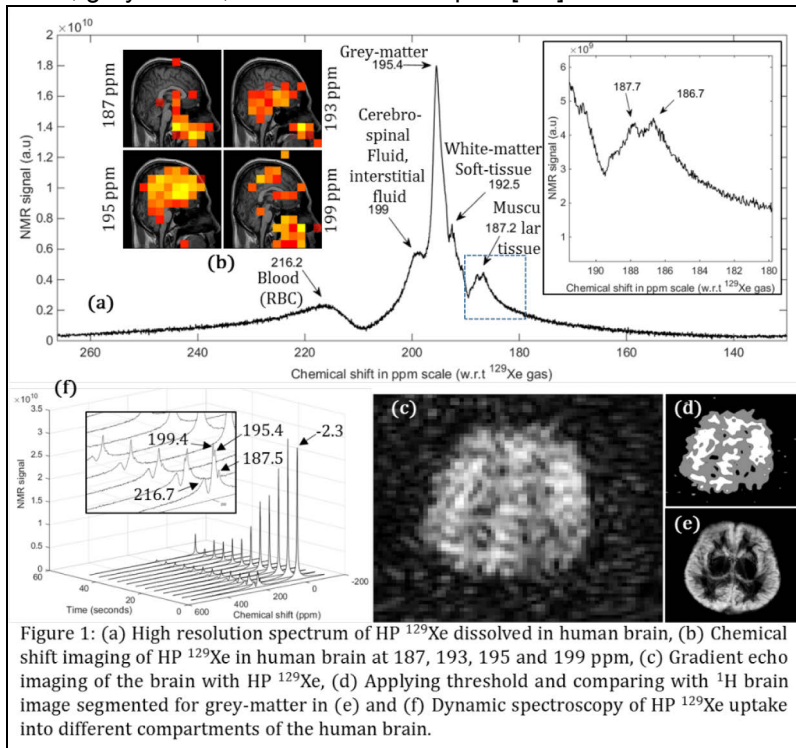
## Talk 10

### MR imaging and spectroscopy of human brain with hyperpolarized $^{129}\text{Xe}$ at 1.5T

**Madhwesha Rao, Neil J Stewart, Graham Norquay, Paul D Griffiths, Jim M Wild**

Academic unit of radiology, University of Sheffield, UK

**Purpose:** When inhaled, Xenon dissolves in the blood, is carried to the brain where it crosses the blood-brain barrier (BBB) and dissolves in brain tissues. The wide chemical shift range of  $^{129}\text{Xe}$  provides contrast to different compartments of the brain: the cerebral blood, grey-matter, white-matter and lipids [1-4].



**Motivation:** To (a) demonstrate hyperpolarized (HP)  $^{129}\text{Xe}$  as a safe, non-invasive contrast agent for imaging xenon (blood) delivery to the human brain and (b) investigate  $^{129}\text{Xe}$  as a physiological marker of BBB integrity.

**Methods:** An 8-leg birdcage coil tuned to the  $^{129}\text{Xe}$  (17.6 MHz) was constructed. In-vivo spectroscopy and imaging of HP  $^{129}\text{Xe}$  dissolved in the human brain was performed at 1.5 T (GE Signa HDx).  $^{129}\text{Xe}$  gas was HP by spin exchange optical pumping [5] and 1 L doses were inhaled by healthy subjects. 2D gradient-echo images of HP  $^{129}\text{Xe}$  in the brain were acquired at three separate time-points (8s, 16s and 24s after inhalation) and averaged. Subjects tolerated the breath-hold well and vital signs were monitored throughout the scan. The infusion of HP  $^{129}\text{Xe}$  into human is driven by (a) concentration gradient and (b) diffusive exchange. We developed a model to determine the exchange-fraction (F) between tissue (depolarized  $^{129}\text{Xe}$ ) and blood (HP  $^{129}\text{Xe}$ ), which depends on the intrinsic characteristics of the BBB (permeability, total perfused surface area).

**Results:** HP  $^{129}\text{Xe}$  spectra exhibited several peaks in the human brain (Fig1(a)). Linking these to the spatial location (via chemical-shift imaging Fig(b)) we attributed the peaks to  $^{129}\text{Xe}$  dissolved in cerebral blood (216ppm), grey-matter (196ppm), white-matter (192ppm), CSF & interstitial-fluid (199ppm) and soft muscular tissue (187ppm). Fig1(c) is a 2D axial gradient-echo image of HP  $^{129}\text{Xe}$  dissolved in the human brain. Thresholding the image in Fig1(c) we arrive at Fig1(d) which correlates well with the structural information from the  $^1\text{H}$  grey-matter images (Fig1(e)). Fig1(f) depicts the dynamics of HP  $^{129}\text{Xe}$  uptake in human brain. The developed model estimates the exchanging fraction  $F \approx 0.1\text{s}^{-1}$  (10%).

**Discussion:** We have demonstrated human brain imaging with HP  $^{129}\text{Xe}$  for the first time. With models of tracer kinetics the dynamics of HP  $^{129}\text{Xe}$  uptake in human brain tissue can be used to access the physiological integrity of the BBB.

#### References:

- [1]. W. Kilian, et al, MRM, 51 (2004), 843-47.
- [2]. W. Kilian, et al, Proc. Int. Soc. Magn. Reson. Med. 13 (2005); ISSN 1545-4436 [3]. K. Nakamura, et al, MRM, 53 (2005), 528-34.
- [4]. J. P. Mugler Iii, et al, MRM, 37 (1997), 809-15. [5]. G. Norquay, et al., JAP, 113 (2013).

## Talk 11

# Magnetic Resonance Imaging of Hyperpolarized Xenon-129 in the Brain

Mitchell S. Albert,<sup>1,2</sup> Francis Hane,<sup>1,2</sup>

<sup>1</sup> Lakehead University, 955 Oliver Rd, Thunder Bay, Canada

<sup>2</sup> Thunder Bay Regional Research Institute, 980 Oliver Rd, Thunder Bay Canada

### Introduction

Hyperpolarized (HP) gas magnetic resonance imaging (MRI) takes advantage of the hyperpolarizability of inert gases such as  $^3\text{He}$  and  $^{129}\text{Xe}$  which allows signal-to-noise ratios (SNR) that are several orders of magnitude in excess of their thermally polarized forms. Albert et al. first demonstrated biological HP gas MRI in initial work conducted on lungs [1]. However xenon has unique anesthetic properties which make it ideally suited for studies in the brain. These studies include the imaging of ischemic areas in the brain in stroke victims and as a functional brain imaging modality to detect pain [6,7].

### T1 Relaxation in the Brain

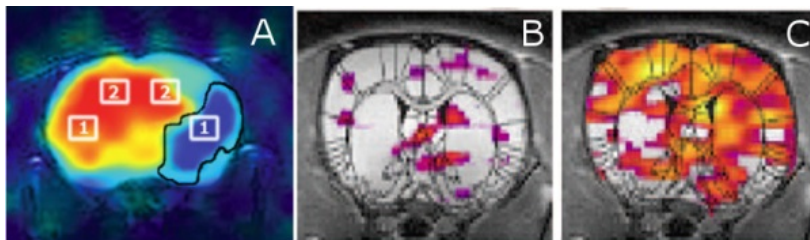
One of the major challenges of using HP  $^{129}\text{Xe}$  is the relatively short spin-lattice relaxation time (T1) of  $^{129}\text{Xe}$  in the blood. The T1 for  $^{129}\text{Xe}$  has been measured to be about 4 s in deoxygenated blood and about 8 s in oxygenated blood [2,3]. T1 time is considerably longer in the brain, about 15 s, making brain imaging using  $^{129}\text{Xe}$  possible [4]. The short T1 *in vivo* makes consecutive scans difficult, but the T1 falls within the blood transport time and permits the successful acquisition of brain images [5].

### Stroke Imaging using hyperpolarized xenon

Ischemic stroke occurs because of an occlusion in the cerebrovasculature. Because HP  $^{129}\text{Xe}$  is dissolved in the blood flow, a stroke is detectable using HP gas MR imaging. Using this novel imaging modality, we demonstrated the detection of ischemic stroke in a mouse stroke model (Fig. A) [6].

## Function MRI of pain using hyperpolarized xenon

We have demonstrated HP gas MRI as a functional imaging modality by imaging the rat brain when exposed to a chemical pain stimulus. In these experiments, we injected the mouse with the pain stimulating compound capsaicin and observed higher  $^{129}\text{Xe}$  signal in the brain of rats exposed to the pain stimulus (Fig. C) than before stimulation (Fig. B) [7].



### References:

- [1] M. Albert, G. Cates, B. Driehuys, et al, *Nature*, **370** (1994) 199.
- [2] M. Albert, D. Kacher, D. Balamore, et al, *J Magn Reson*. **140**, (1999) 264.
- [3] M. Albert, et al, *NMR in Biomed*. **13**, (2000) 407; J. Wolber, Bifone, et al, *MRM*, **46**, (2001) 586.
- [4] X. Zhou, M. Mazzanti, J. Chen, et al, *NMR Biomed*, **21**, (2008) 217.
- [5] J. Nouis, Z. I. Cleveland, B. Driehuys, et al, *Proc. ISMRM*, (2011)
- [5] X. Zhou, Y. Sun, M. Mazzanti, et al, *NMR Biomed*, **24**, (2011), 170.
- [6] M. Mazzanti, R. Walvick, X. Zhou, et al, *PLoS ONE*, **6**, (2011), e21607.

## Talk 12

### **New developments related to fast and multiplexed detection of $^{129}\text{Xe}$ NMR biosensors**

**P. Berthault,<sup>1</sup> C. Boutin,<sup>1</sup> G. Carret,<sup>1</sup> J.-P. Dognon,<sup>2</sup> E. Léonce,<sup>1</sup>  
E. Mari<sup>1</sup>**

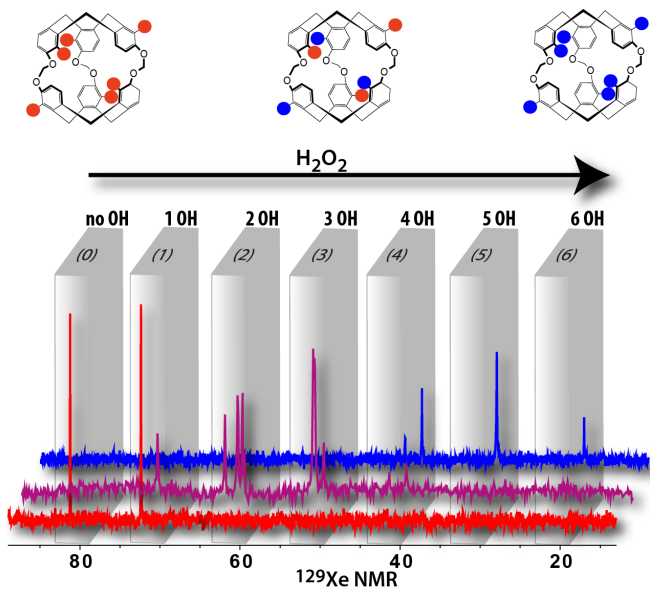
CEA Saclay, IRAMIS, NIMBE, UMR CEA/CNRS 3685, 91191 Gif sur Yvette, France.

<sup>1</sup> Laboratoire Structure et Dynamique par Résonance Magnétique

<sup>2</sup> Laboratoire de Chimie Moléculaire et de Catalyse pour l'Energie

The use of biosensors made of dedicated xenon host systems bearing suitable ligands is a recent domain in vast expansion. The richness of the approach lies in the specific spectral signature offered to hyperpolarized xenon when encapsulated in such hosts and the continuous in-out xenon exchange.

In order to reach low detection thresholds, progresses have been made in the production and delivery of laser-polarized xenon,[1] in the design of 'smart' (target-responsive) and/or bimodal probes [2] as well as in the use of quantum chemistry to predict the xenon chemical shifts,[3] and finally in the development of fast NMR/MRI methods taking full profit of the hyperpolarization.[4] Some of these aspects will be presented.



$^{129}\text{Xe}$  NMR spectra recorded after addition of  $\text{H}_2\text{O}_2$  to a solution of a cryptophane bearing boronate groups, showing the progressive evolution of the xenon chemical shifts as the boronate groups are transformed into OH groups.

#### References:

- [1] A. Causier et al., Lab Chip **15** (2015) 2049 - 2054
- [2] N. Kotera et al., Chem. Comm. DOI: 10.1039/C5CC04721H.
- [3] E. Dubost et al., Angew. Chem. **53** (2014) 9837-9840.
- [4] C. Boutin et al., J. Phys. Chem. Lett. **4** (2013) 4172-4176.

## Talk 14

### Investigation of Differences in Diastereomeric Chemical Shift Response to Metal Ion Chelation by 129-Xenon NMR

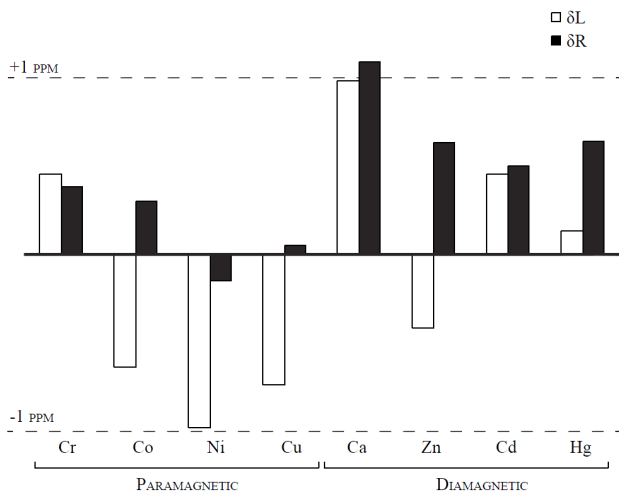
C. Slack<sup>1</sup>, K. Jeong<sup>1</sup>, C. Vassiliou<sup>1</sup>, A. Truxal<sup>1</sup>, P. Dao<sup>1</sup>, M. Gomes<sup>1</sup>, M. Francis<sup>1</sup>, D. Wemmer<sup>1</sup>, A. Pines<sup>1,2</sup>

<sup>1</sup>University of California, Berkeley, United States

<sup>2</sup>Material Sciences Division Lawrence Berkeley National Lab, Berkeley, United States

Creating a better sensor for metal ion detection could be useful across a wide range of fields including medical diagnostics and environmental toxicology. The shifts induced by  $\text{Ca}^{2+}$ ,  $\text{Cu}^{2+}$ ,  $\text{Dy}^{3+}$ ,  $\text{Zn}^{2+}$ ,  $\text{Cd}^{2+}$ ,  $\text{Ni}^{2+}$ ,  $\text{Co}^{2+}$ , and  $\text{Hg}^{2+}$  binding to a DOTA bound to cryptophane are distinct to each metal, and diastereomer. In addition the different responses of the diastereomers for the same metal ion indicate that shifts are affected by partial folding, with a correlation between expected coordination number of the metal in the DOTA complex and 129Xe chemical shift (shown below). DOTA is a flexible chelation agent with eight possible coordination points, four tertiary amines in the central ring and four carboxylate arms. The geometry of the metal bound DOTA is dependent on the specific metal present, and its preferred coordination number, CN. For 9 coordinate complexes that incorporate a water molecule as a cap there has also been an observed chirality similar to the one observed for cryptophane [1]. By investigating multiple structures with the DOTA moiety shifted down the solubilizing peptide chain we can get a better understanding of affect of the different properties of the metals on the observed chemical shift for each diastereomer. A more complete understanding of the details may allow further optimization for maximal response and utility for cryptophane based sensors across all applications.





### References:

- [1] Aime, S.; Botta, M.; Fasano, M.; Paula, M.; Marques, M.; Geraldes, C. F. G. C.; Pubanz, D.; Merbach, A. E. *Inorg. Chem.* **36** (1997) 2059-2068.

## Talk 15

### Sensors based on polarized noble gasses

A. Palacios-Laloy<sup>1</sup>

<sup>1</sup> Innovative sensors lab, CEA-LETI, 17 avenue des Martyrs, 38000 Grenoble

Optically-pumped magnetometers rely on spin-polarized species to measure magnetic fields. The most common configurations use electronic polarized atoms (alkali or helium-4) and address numerous applications going from biomed (magneto-cardiography and magneto-encephalography), to geophysics and magnetic anomaly detection for submarine warfare.

Our laboratory has been working for more than a decade on scalar helium-4 magnetometers for space applications. Thanks to a specific configuration based on spin alignment rather than orientation and keeping the laser polarization orthogonal to the magnetic field we have been able to reach unprecedented levels of absolute precision. A miniaturized variant, providing vector sensitivity is currently being developed for biomed applications [1,2].

Noble gasses polarized by spin exchange constitute a valuable asset for magnetometry and gyroscopy. I will introduce magnetometers based on hyperpolarized helium-3, and a more recent proposition on the combination of an alkali and a noble gas. On the field of gyroscopy, NMR gyroscopes, which measure the rotation as a differential effect in the precession of two nuclear spins, began using hyperpolarized noble gasses in the 1970s. At that time their development yielded important fundamental results on spin-exchange optical pumping. Recent advances on miniaturization of clocks and magnetometers, and, the invention in Princeton of an elegant alternative: the co-magnetometer [3] triggered new interest for these gyroscopes. I will introduce the physical principles and the main challenges which need to be addressed by these technologies to build a navigation-class sensor in the near future.

#### References:

- [1] J. Rutkowski et al., *Sensors and Actuators A: Physical* **216** (2014) 386.
- [2] M.-C. Corsi, et al., *Biomag 2014*, Aug 2014, Halifax.
- [3] E. A. Donley, *2010 IEEE Sensors* (2010) 17.

**Notes:**

## Talk 16

### **3D-printed system optimizing dissolution of hyperpolarized gaseous species for micro-sized NMR**

**C. Boutin<sup>1</sup>, A. Causier<sup>1,2</sup>, G. Carret<sup>1</sup>, T. Berthelot<sup>2</sup> and P. Berthault<sup>1</sup>**

CEA Saclay, IRAMIS, NIMBE, UMR CEA/CNRS 3685, 91191 Gif sur Yvette, France.

<sup>1</sup> Laboratoire Structure et Dynamique par Résonance Magnétique,

<sup>2</sup> Laboratoire d'Innovation en Chimie des Surfaces et Nanosciences

Dissolution of hyperpolarized species in liquids of interest for NMR is often hampered by the presence of bubbles that degrade the field homogeneity. We describe here a system using a microfluidic device for continuous- or stopped-flow delivery of gas (Figure 1), enabling its dissolution into a small volume as close as possible to the detection region for optimized magnetic resonance spectroscopy and imaging. [1] We have developed a compact system that can be integrated into a conventional narrow-bore magnet in order to work with the high and homogeneous magnetic fields required for spectral resolution but also to reduce the sample volume.

We show that direct fabrication of 3D structures as milli/microfluidic systems by additive technologies such as 3D printing presents advantages such as fast and costless development with high achievable resolution on various materials, allowing rapid prototyping for a specific application such as spin noise experiments or experiments with living biological cells. The problems related to cleanroom techniques are avoided

The proof-of-concept made via hyperpolarized <sup>129</sup>Xe NMR experiments reveals high and homogeneous dissolution of the gas in water.

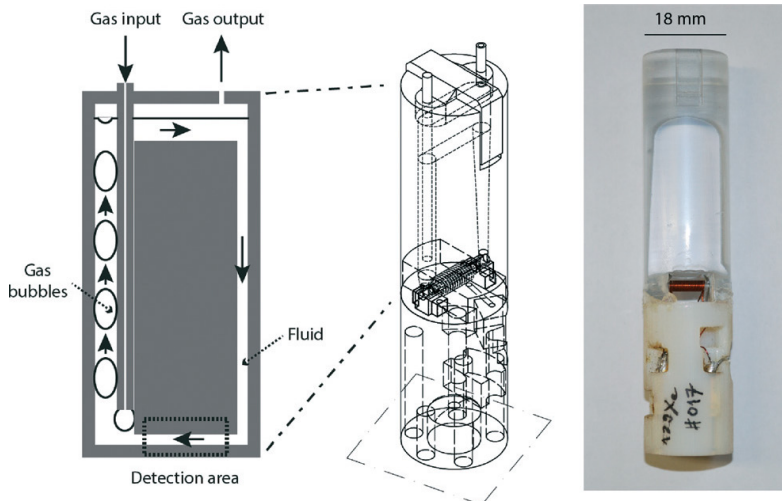


Figure 1: The NMR cell. The principle of the bubble pump (in its top part) is depicted on the left. Middle: 3D drawing of the whole cell. Right: picture of one of these cells equipped with a  $^{129}\text{Xe}$  solenoid coil.

### References:

- [1] A. Causier, G. Carret, C. Boutin, T. Berthelot and P. Berthault, Lab on a Chip. 15 (2015) 2049-2054.

## Talk 17

# Pulmonary oxygenation determination using hyperpolarised $^{129}\text{Xe}$ NMR

G. Norquay,<sup>1</sup> N. J. Stewart,<sup>1</sup> J. M. Wild<sup>1</sup>

<sup>1</sup>University of Sheffield, Sheffield, South Yorkshire, United Kingdom

**Purpose:** In this work, a method for direct, non-invasive dynamic measurement of pulmonary oxygenation *in vivo* using hyperpolarised (HP)  $^{129}\text{Xe}$  NMR is demonstrated.

**Method:** *In vitro experiments:* for NMR acquisition at 1.5 T and 3 T, pulse-acquire sequences were used with block pulses (500  $\mu\text{s}$ ), receive bandwidths of 2.5 kHz (1.5 T) and 4 kHz (3 T) and an inter-pulse delay (TR) of 0.5 s. The chemical shift of the  $^{129}\text{Xe}$  red blood cell resonance was explored as a function of  $\text{sO}_2$  following experimental methods in [1]. *In vivo lung spectroscopy:* Two healthy subjects inhaled 600 mL of HP  $^{129}\text{Xe}$  and performed a 45 s breath-hold on a clinical 3 T MR scanner. Pulse-acquire NMR measurements (FA =  $90^\circ$ , centred on the  $^{129}\text{Xe}$ -RBC resonance) were performed over the whole lungs with a receive bandwidth of 3 kHz, 2048 samples (freq. resolution = 0.04 ppm) and TR of 0.8 s. The experiment was repeated with increased temporal resolution (TR = 0.1 s), by reducing the sampling to 128 points (freq. resolution = 0.7 ppm). The amplitude of the detected  $^{129}\text{Xe}$ -RBC and  $^{129}\text{Xe}$ -tissue/plasma (TP) signals *in vivo* were

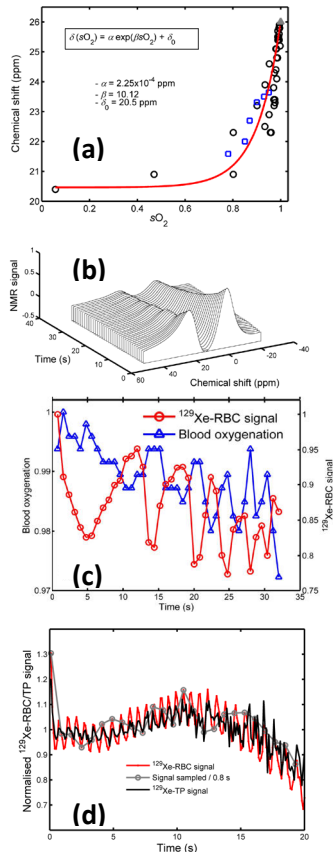


Fig.1: (a) *In vitro* calibration curve. (b) *In vivo* breath-hold decaying spectra. (c) Pulmonary blood oxygenation and  $^{129}\text{Xe}$ -RBC signal vs. Breath-hold time (TR = 0.8 s). (d)  $^{129}\text{Xe}$ -RBC/TP signal vs breath-hold time (TR = 0.1 s)

normalised to the  $^{129}\text{Xe}$  gas  $T_1$  decay in the lungs (measured as 18 s).

**Results and Discussion:** *In vitro data:* the  $^{129}\text{Xe}$ -RBC chemical shift increased non-linearly with increasing  $s\text{O}_2$  (Fig. 1 (a)). The  $^{129}\text{Xe}$ -plasma peak position remained fixed for all  $s\text{O}_2$  values. *In vivo data:* with TR = 0.8 s, the amplitude of the  $^{129}\text{Xe}$ -RBC signal oscillated over the breath-hold with a time period of  $\sim 1$  s. In addition, the pulmonary blood oxygenation, calculated by converting the measured *in vivo*  $^{129}\text{Xe}$ -RBC chemical shift into oxygenation using the *in vitro* data for calibration (Fig. 1 (c)), oscillated at the same frequency as the  $^{129}\text{Xe}$ -RBC signal, suggestive of a link between pulmonary oxygenation and cardiac output. Ruppert *et al.*, [2] previously observed  $^{129}\text{Xe}$ -RBC (and  $^{129}\text{Xe}$ -TP) signal modulations (peak-to-peak period of  $\sim 1$  s, TR of 0.1 s), and attributed this behavior to cardiac pulsation. The dataset acquired at increased temporal resolution (TR = 0.1 s, Fig. 1, (d)), confirmed the observations of Ruppert *et al.*, where the  $^{129}\text{Xe}$ -RBC and  $^{129}\text{Xe}$ -TP signals oscillated at rates of the same order as cardiac pulsation. For TR = 0.1 s, the freq. resolution (0.7 ppm) was not sufficient to discriminate changes in the  $^{129}\text{Xe}$ -RBC peak position (and hence oxygenation) over the breath-hold duration. To overcome this limitation, further work with cardiac gating acquisitions is underway to probe  $^{129}\text{Xe}$ -RBC chemical shifts (blood oxygenations) at specific time points, thereby enabling real-time monitoring of pulmonary oxygenation throughout the cardiac cycle.

### **References:**

- [1] Norquay *et al.*, MRM doi:10.1002/mrm.25417, 2014. [2] Ruppert *et al.*, ISMRM, 0817, 2013.

## Talk 18

# Functionalized Xenon for Cellular Labelling in $^{129}\text{Xe}$ MRI: Biosensor Design for High Sensitivity and Specificity

Leif Schröder,<sup>1</sup>

<sup>1</sup> Leibniz-Institut für Molekulare Pharmakologie (FMP), Robert-Rössle-Str.  
10, 13125 Berlin, Germany

Supramolecular xenon hosts were first proposed in 2001 as a method to functionalize the NMR signal of  $^{129}\text{Xe}$  for implementing hyperpolarized sensors [1] that serve as a platform to design ultra-sensitive targeted contrast agents for diagnostic imaging. While the design of the host structure made early advancements in terms of optimized cryptophane cages, demonstrations of MRI studies on live cells with different biosensor labelling status was achieved only recently [2]. This presentation will give an overview of recent advancements in delivery of hyperpolarized Xe to enable live cell studies and different approaches in sensor design to combine high sensitivity and high specificity. Efficient labelling of target versus control cells is demonstrated with an antibody-based approach [3] and through biorthogonal click chemistry in metabolic oligosaccharide engineering [4]. This already allows MRI detection at nanomolar sensor concentrations and can address molecular targets that are rather challenging for conventional relaxivity-based contrast agents. Further sensitivity enhancement can be achieved by implementing a high local cage concentration at the molecular targeting side, e.g. through targeted liposomal vesicles characterized by a high Xe host load [5]. Some of these approaches can be considered as development platforms with a convenient flexibility to address various targets. Altogether, xenon biosensors continue in improving their outstanding sensitivity and their diagnostic value while the field is in transition to first biomedical applications.



## References:

- [1] M. M. Spence, S. M. Rubin, I. E. Dimitrov, E. J. Ruiz, D. E. Wemmer, A. Pines, S. Q. Yao, F. Tian, P. G. Schultz, *Proc. Natl. Acad. Sci. U.S.A.* **98** (2001) 10654-10657
- [2] S. Klippel, J. Döpfert, J. Jayapaul, M. Kunth, F. Rossella, M. Schnurr, C. Witte, C. Freund, L. Schröder, *Angew. Chem. Int. Ed.* **53** (2014) 493-496
- [3] H. M. Rose, C. Witte, F. Rossella, S. Klippel, C. Freund, L. Schröder, *Proc. Natl. Acad. Sci. U.S.A.* **111** (2014) 11697-11702
- [4] C. Witte, V. Martos, H. M. Rose, S. Reinke, S. Klippel, L. Schröder, C. P. R. Hackenberger, *Angew. Chem. Int. Ed.* **54** (2015) 2806-2810
- [5] M. Schnurr, K. Sydow, H. M. Rose, M. Dathe, L. Schröder, *Adv. Healthcare Mat.* **4** (2015) 40-45

## Talk 19

### Multiparametric Evaluation of COPD by Hyperpolarized Xenon ADC and CEST MRI

Haidong Li, Zhiying Zhang, Weiwei Ruan, Jianping Zhong,  
Xiuchao Zhao, Xianping Sun, Chaohui Ye, Xin Zhou\*

Key Laboratory of Magnetic Resonance in Biological Systems, State Key Laboratory of Magnetic Resonance and Atomic and Molecular Physics, National Center for Magnetic Resonance in Wuhan, Wuhan Institute of Physics and Mathematics, Chinese Academy of Sciences, Wuhan, 430071, China. (\*Email: xinzhou@wipm.ac.cn)

Diffusing capacity is the essential function of the lung, which is usually evaluated in clinic by pulmonary function tests (PFTs). However, the regional information of diffusion in the lung can not be quantified by PFTs. Hyperpolarized (HP) xenon MR opens a new door to study the lung structure and function, due to its extremely high MR sensitivity, good solubility and chemical shift sensitivity [1-5]. In our study, we quantitatively evaluate both pulmonary microstructure and pulmonary diffusing capacity in the COPD rats by using HP xenon apparent diffusion coefficient (ADC) and chemical exchange saturation transfer (CEST) MRI.

All COPD rat models were induced by exposure to second-hand smoke and lipopolysaccharide (LPS). A single b value ( $b=14 \text{ s/cm}^2$ ) diffusion-weighted hyperpolarized  $^{129}\text{Xe}$  MRI sequence was used for higher image SNR. The mean lung parenchymal  $^{129}\text{Xe}$  ADC of  $0.04422 \pm 0.0029$  and  $0.04234 \pm 0.0023 \text{ cm}^2/\text{s}$  ( $\Delta=0.8/1.2 \text{ ms}$ ) for COPD rats showed a significant increasement compared to that of  $0.0377 \pm 0.0023$  and  $0.0367 \pm 0.0013 \text{ cm}^2/\text{s}$  ( $\Delta=0.8/1.2 \text{ ms}$ ) for healthy rats. The corresponding ADC histogram of COPD rats exhibited a moderately broader distribution. It indicated that the microstructure of alveolar airspace was enlarged in COPD rats.

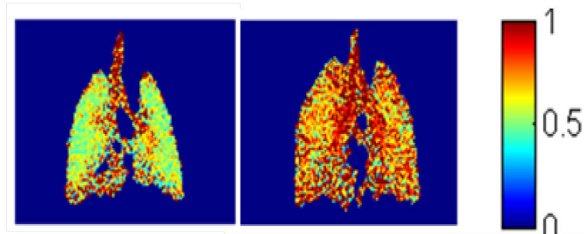


Fig. 1. The diffusion time constant distribution in healthy (left) and COPD (right) rats lung.

Dynamic CEST spectra and MR images were used to quantitatively evaluate the global and local diffusing capacity in the lung, respectively. Typical xenon gas signal dynamics in the lung were exponential (now shown), and the significant difference of decay parameter was found between the healthy and COPD rats. The diffusion time constant for COPD rats was  $0.88 \pm 0.16$  s, which increased significantly ( $P = 0.001$ ) compared with that in the healthy ones ( $0.60 \pm 0.07$  s). The higher diffusion time constant in the trachea was observed in both healthy and COPD rats (shown in Fig. 1), because gas exchange mainly occurs in the alveoli of the lung. Compared with the healthy rat, the diffusion time constant in the COPD was obviously increased in the parenchyma, because the gas exchange function was destroyed.

HP xenon ADC and CEST MRI are able to quantitatively depict both pulmonary microstructure and global/local pulmonary diffusing capacity, providing a multiparametric method to evaluate not only the COPD, but also other lung diseases.

#### References:

- [1] D. Yablonskiy, A. Sukstanskii, et. al., *Magn. Reson. Med.* **71** (2014) 486.
- [2] S. Kaushik, Z. Cleveland, et. al., *Magn. Reson. Med.* **65** (2011) 1155.
- [3] M. Boudreau, X. Xu, et. al., *Magn. Reson. Med.* **69** (2013) 211.
- [4] K. Ruppert, J. Brookeman, et. al., *Magn. Reson. Med.* **44** (2000) 349.
- [5] B. Driehuys, G. Cofer, et. al., *Proc. Nat. Acad. Sci. USA*, **103** (2006) 18278.

## Talk 20

### Methods for hyperpolarised xenon MR imaging of the human lungs and brain

Neil J Stewart, Graham Norquay, Madhwesha Rao, Jim M Wild

Academic Unit of Radiology, University of Sheffield, Sheffield, UK

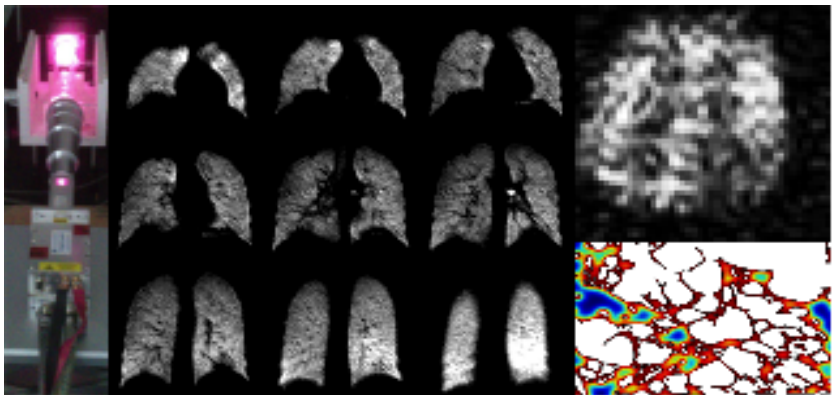
This invited talk will cover recent research methodology and technological developments from the Sheffield group for improving the sensitivity of  $^{129}\text{Xe}$  MR for functional imaging of the lungs and brain in humans.

The talk will cover aspects of:

- Developments in polarisation of  $^{129}\text{Xe}$  by SEOP for large-scale production of hyperpolarised xenon for in vivo applications.
- RF hardware and  $B_0$  field strength related considerations for optimising the sensitivity of human lung MRI with  $^{129}\text{Xe}$ .
- Pulse sequence strategies for enhanced SNR lung imaging with  $^{129}\text{Xe}$  and image acceleration techniques exploiting steady state free precession, parallel imaging, under-sampled non-Cartesian trajectories and compressed sensing.
- Customised pulse sequence design for functional lung imaging with hyperpolarised  $^{129}\text{Xe}$ , including: volumetric acquisition of lung ventilation, gas flow, diffusion and gas exchange information, among other aspects of lung function.
- Technological developments for the simultaneous capture of MR signals from multiple nuclei.

- Mathematical models of  $^{129}\text{Xe}$  MR signal in lung and brain that offer insight into pathophysiology.
- Recent results from spectroscopy and imaging studies of  $^{129}\text{Xe}$  in human brain.

The talk will be illustrated with results of current research from the Sheffield lab. Examples of how the techniques are being used in clinical research / clinical practice will be highlighted.



## Talk 21

### An Expanded Palette of Xenon Biosensors

Y. Wang,<sup>1</sup> B.A. Riggle,<sup>1</sup> B. Roose,<sup>1</sup> I.J. Dmochowski<sup>1</sup>

<sup>1</sup> Univ. Pennsylvania, Department of Chemistry, 231 South 34<sup>th</sup> St., Philadelphia, PA 19104 USA

Hyperpolarized (HP) <sup>129</sup>Xe chemical exchange saturation transfer (Hyper-CEST) NMR methods have enabled the detection of cryptophane organic host molecules [1-3], protein vesicles, lipid vesicles, and bacterial spores [4] at sub-micromolar concentrations. In Hyper-CEST, encapsulated HP <sup>129</sup>Xe is selectively depolarized by radiofrequency (rf) pulses, and the depolarized <sup>129</sup>Xe rapidly exchanges with HP <sup>129</sup>Xe to accumulate in the solvent pool, where loss of signal can be readily monitored (Figure 1). Cryptophane-A and its derivatives are the most studied Xe-binding hosts, and they exhibit the highest measured affinity for xenon. However, lack of available biosensors has limited the broad application of Hyper-CEST NMR, as functionalized cryptophanes require multi-step synthesis and are isolated in low yields. This has motivated our search for new molecular scaffolds for xenon, to advance applications in sensing, biophysical chemistry, and biomedical imaging. Herein, commercially available cucurbit[6]uril (CB[6], Figure 1) is shown to serve as an ultrasensitive <sup>129</sup>Xe NMR contrast agent and biosensor [5]. CB[6] can be employed as both a “turn off” and “turn on” biodetection agent. In studying host molecules engaged in Hyper-CEST NMR, we have learned that near-optimal, room-temperature xenon exchange rate ( $k_{\text{exch}} \approx 1$  kHz) can contribute even more significantly than Xe affinity to overall detection sensitivity using standard NMR pulse sequences, provided the <sup>129</sup>Xe-host chemical shift is well-resolved spectrally from the <sup>129</sup>Xe-H<sub>2</sub>O peak. This concept makes accessible new classes of low-affinity Xe host molecules, including genetically encoded biosensors.

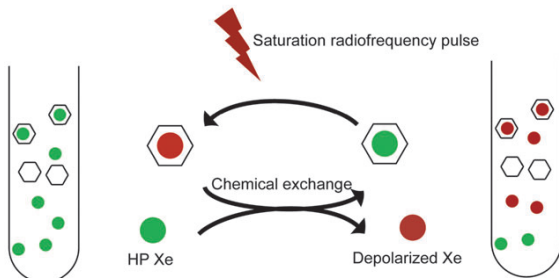
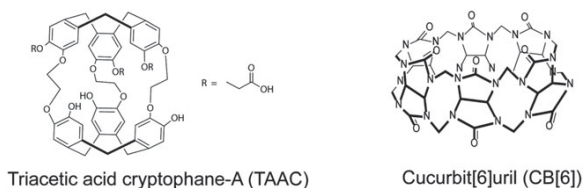


**Figure 1.** Top: chemical structures of CB[6] and TAAC. Bottom: HyperCEST mechanism involving xenon-binding molecules represented by hexagons.

**References:**

- [1] L. Schroeder, T.J. Lowery, C. Hilty, D.E. Wemmer, A. Pines, *Science* **314** (2006), 446-449.
- [2] Y. Bai, A.P. Hill, I.J. Dmochowski, *Anal. Chem.* **84** (2012), 9935-9941.
- [3] B.A. Riggle, Y. Wang, I.J. Dmochowski, *J. Am. Chem. Soc.*, **137** (2015), 5542-5548.
- [4] Y. Bai, Y. Wang, A. Driks, M. Goulian, I.J. Dmochowski, *Chem Sci.*, **5** (2014), 3197-3203.
- [5] Y. Wang, I.J. Dmochowski, *Chem. Comm.* **51** (2015), 8982-8985.

## Talk 22

# Genetically Encoded Reporters for HyperCEST MRI

Mikhail G. Shapiro

Division of Chemistry and Chemical Engineering,  
California Institute of Technology, Pasadena, CA, USA  
shapirolab.caltech.edu

This talk will describe the development of genetically encoded imaging agents for hyperpolarized xenon MRI and their potential applications to *in vivo* biological imaging. These reporters are based on gas vesicles (GVs), a unique class of gas-containing nanostructures formed by certain microorganisms as a means to regulate buoyancy [1]. GVs are hollow protein-shelled compartments ~250 nm in size that exclude water but are permeable to gas. The contents of GVs are in constant exchange with gas molecules dissolved in surrounding media. We recently showed that GVs can interact with dissolved xenon, enabling their imaging with HyperCEST at picomolar concentrations, both in isolation and inside cells [2]. Furthermore, GVs from different host species, which have different shapes and sizes, operate at distinct chemical shifts, enabling multiplexed imaging. We have shown that heterologously expressed GVs can image inducible gene expression in *E. coli*, and that biofunctionalized GVs are able to detect human cancer cells *in vitro*. Ongoing research is focused on genetic engineering of GV physical and biochemical properties for enhanced biodistribution and targeting, heterologous expression in cells that do not natively form GVs, quantitative understanding of GV HyperCEST contrast and modeling and initial implementations of HyperCEST imaging *in vivo*.



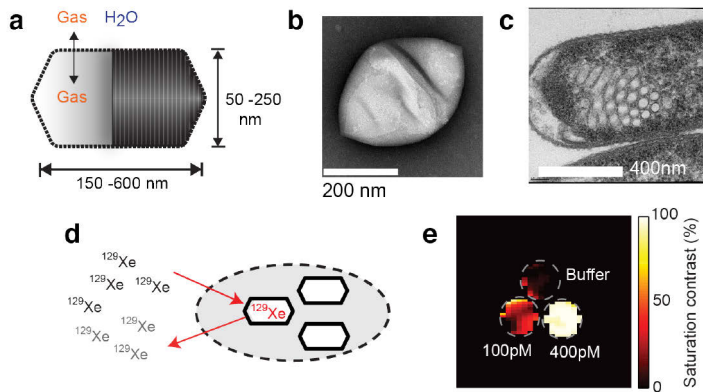


**Figure - Gas Vesicle Xe-MRI.** (a) Diagram of GV structure – a hollow interior formed by a thin gas-permeable protein shell. (b) TEM image of a halobacterial gas vesicle (c) TEM image of GVs expressed in *E. coli*. (d) Hyperpolarized xenon permeates GVs, enabling their detection with HyperCEST. (e) Xe-MRI image of GVs at picomolar concentrations.

### References:

- [1] A. E. Walsby, *Microbiol Rev* **1994**, 58, 94-144.
- [2] M. G. Shapiro et al, *Nature Chemistry* **2014**, 6, 629-34.

## Talk 23

### Systematic improvement of $T_1$ times of HP- $^{129}\text{Xe}$ at low fields

**M. Repetto<sup>1</sup>, E. Babcock<sup>2</sup>, P. Blümler<sup>1</sup>, W. Heil<sup>1</sup>, S. Karpuk<sup>1</sup> and K. Tullney<sup>1</sup> and S. Zimmer<sup>1</sup>**

<sup>1</sup> Johannes Gutenberg University, Staudingerweg 7 55128 Mainz, Germany

<sup>2</sup> Jülich Centre for Neutron Science, Forschungszentrum Jülich GmbH, Outstation at MLZ, Lichtenbergstrasse 1, 85747 Garching, Germany.

Most of the applications of HP-Xe profit from high polarization degrees. Over the last years, many effort was invested in improving the performance of the Xe-polarizers achieving polarization degrees up to 64% [1]. However, these successful results should be complemented by an efficient storage in order to minimize polarization losses. This condition is especially relevant for applications where the HP-Xe must be transported to another facility and/or long spin coherence times are required e.g. experiments with He-Xe co-magnetometers [2]. The highest difficulty so far was to ensure the reproducibility of those storage times.

In this work [3], the spin-lattice relaxation time ( $T_1$ ) of hyperpolarized HP- $^{129}\text{Xe}$  was significantly improved using uncoated, Rb-free, spherical cells made from aluminosilicate glass (GE180). The  $T_1$  was determined in a self-made low field NMR system (20 G) for both: pure HP-Xe and HP-Xe in mixtures with  $\text{N}_2$ ,  $\text{SF}_6$  and  $\text{CO}_2$ . From this experiment, the van der Waals relaxation [4,5] for pure Xe (with 85%  $^{129}\text{Xe}$ ) was found to be  $(4.6 \pm 0.1)$  h and typical wall relaxation times of about 18 h were founded for 10 cm in diameter glass cell. Furthermore, it was found that especially  $\text{CO}_2$  exhibited an unexpected high efficiency in shortening the lifetime of the Xe-Xe dimers and hence prolonging the total  $T_1$ .

During this experiment, an “aging” process of the wall relaxation was identified by performing measurements on the same cell. This effect could be easily removed by repeating the initial cleaning procedure. In this way, a constant wall relaxation was ensured over all the experiments. Finally, the van der Waals relaxation for HP-Xe in natural abundance was determined in mixtures with  $\text{SF}_6$ . Surprisingly, this value turned out to be about 75% shorter when compared to that found for Xe with 85% isotopic enrichment.

## References:

- [1] I.C. Ruset, S. Ketel, F.W. Hersman, *Phys. Rev. Lett.* **96** (2006) 053002-053004.
- [2] K. Tullney, F. Allmendinger, M. Burghoff, *Phys. Rev. Lett.* **111** (2013) 100801-100805.
- [3] M. Repetto, E. Babcock, P. Blümler, *Jour. of Mag. Res.* **252** (2015), 163-169
- [4] B. Chann, I.A. Nelson, L.W. Anderson, *Phys. Rev. Lett.* **88** (2002) 113201-113204.
- [5] B.C. Anger, G. Schrank, A. Schoeck, *Phys. Rev. A* **78** (2008) 043406-043410.

## Talk 24

# Relaxation Weighted MRI contrast with Hyperpolarized $^{83}\text{Kr}$ and $^{129}\text{Xe}$ .

T. Meersmann

Sir Peter Mansfield Imaging Centre, Division of Respiratory Medicine, School of Medicine, University of Nottingham, Nottingham, NG7 2RD, United Kingdom

Typically, attempts are made to reduce relaxation of the precious hyperpolarized (hp) spin state and the associated signal loss. For example, paramagnetic metal centers are avoided for hp MRI probes, with a few notable exceptions where the generation of negative contrast through shortened  $T_1$ ,  $T_2$ , or  $T_2^*$  times was exploited [1, 2].

However, our group has made significant progress with hp  $^{83}\text{Kr}$ , a stable, nuclear spin  $I = 9/2$  isotope that according to 'common wisdom' was an unlikely candidate for hp MRI applications because of its fast quadrupolar relaxation [3]. The apparent disadvantage can be turned into a useful probe for surfaces, as quadrupolar relaxation requires the presence of fluctuating electric field gradients (EFGs) that are predominately generated during adsorption on surfaces (see Fig. 1A). Recently, we demonstrated  $^{83}\text{Kr}$  surface quadrupolar relaxation (SQUARE)  $T_1$  maps of an emphysema model in excised rodent lungs [4].

Relaxation may also enable molecular sensing using switchable hp  $^{129}\text{Xe}$  relaxation. In a proof-of-concept study our group has shown that the relaxivity of **Gadolinium**<sup>III</sup>-DOTA on  $^{129}\text{Xe}$  in the solvent increased eightfold through tethering of the paramagnetic molecule to a cryptophane cage (see Fig. 1B). This potent relaxation agent can be 'turned off' specifically for  $^{129}\text{Xe}$  through chemical reactions that spatially separate the **Gd**<sup>III</sup> centre from the attached cryptophane cage [5]. Unlike  $^{129}\text{Xe}$  chemical shift based sensors, the new concept does not require high spectral resolution and may lead to a new generation of responsive contrast agents for molecular MRI.

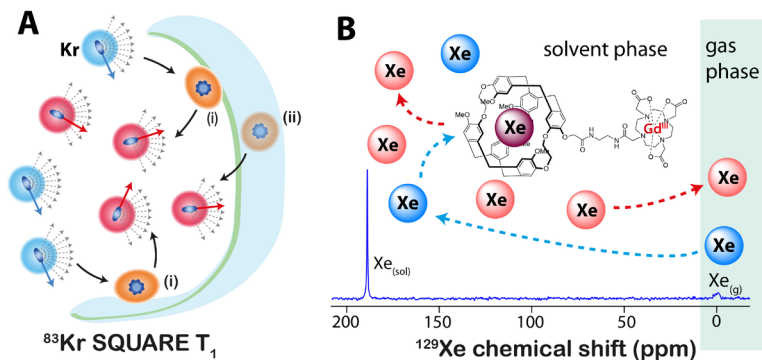


**Fig. 1:** (A) Sketch of surface quadrupolar relaxation (SQUARE) with hp  $^{83}\text{Kr}$ . The krypton atoms experience a fluctuating electron cloud distortion that creates EFGs predominantly during surface adsorption (i) or when dissolved in liquid and tissue below the surface (ii). This causes very fast  $T_1$  relaxation that is transferred via exchange into the gas phase where the effect is observed and MRI contrast is produced. (B) Conceptually similar,  $^{129}\text{Xe}$  experiences fast relaxation while contained for brief time periods within a cryptophane cage tethered to a paramagnetic metal complex (see also recent work by Pines, Wemmer, and co-workers [2]). Chemical exchange relaxation transfer leads to increased relaxation observed in solution (or the gas phase phase). Separation of cage from the paramagnetic metal deactivates this relaxation agent, thus enabling molecular sensing.

### References:

- [1] R. T. Branca *et al.*, P Natl Acad Sci USA **107** (2010).
- [2] M. Gomes *et al.*, in *56th Experimental NMR Conference, April 19 - 24* Asilomar, (2015).
- [3] G. E. Pavlovskaya *et al.*, P Natl Acad Sci USA **102** (2005).
- [4] D. M. L. Lilburn *et al.*, J. R. Soc. Interface **12** (2015).
- [5] F. Zamberlan *et al.*, ChemPhysChem **in press** (2015).

## Talk 25

### **A Temporal-Spatial Study of Zeolite Nucleation by Magnetic Resonance of Hyperpolarized Xenon-129 and Transmission Microscopy**

**M.-A. Springuel-Huet,<sup>1</sup> A. Nossov,<sup>1</sup> G. Melinte,<sup>3</sup> V. Georgieva,<sup>2</sup>  
O. Ersen,<sup>3</sup> F. Gueneau,<sup>1</sup> A. Gedeon,<sup>1</sup> A. Palčić,<sup>2</sup> S. Mintova,<sup>2</sup>  
V.Valtchev<sup>2</sup>**

<sup>1</sup> LCMCP, Sorbonne Universités, UPMC Univ Paris 06, CNRS, Collège de France, Laboratoire de Chimie de la Matière Condensée de Paris, 11 place Marcelin Berthelot, 75005 Paris, France.

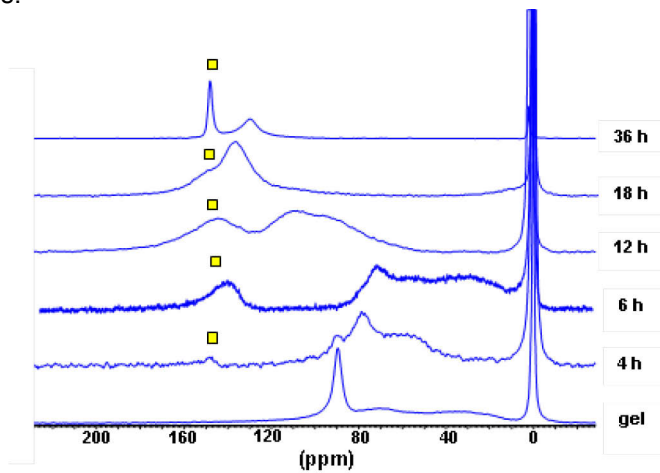
<sup>2</sup> LCS, ENSICAEN – University of Caen - CNRS, 6 Bd Maréchal Juin, 14000 Caen, France

<sup>3</sup> IPCMS, Université de Strasbourg, 23 rue du Loess BP 43, F-67034 Strasbourg, France

The engineering of zeolite materials remains a challenge particularly important nowadays with the changes of the environment protection regulations and of the available fossil hydrocarbons that remain the most important energy sources [1]. Thus, the fine control of zeolite formation is indispensable for the preparation of high quality materials and their further use. A temporal-spatial study of EMT-type zeolite nucleation was performed using a combination of transmission electron microscopy (TEM) techniques and hyperpolarized <sup>129</sup>Xe NMR spectroscopy. The TEM tomography reveals that the initial gel particles exhibit a core-shell structure. The core is filled up with the mother liquor and the shell (about 10-40 nm thick) is dense and non-porous. The set of experimental data revealed that the zeolite nucleation takes place in the shell structure.

<sup>129</sup>Xe NMR spectra recorded at 193 K reveal the presence of the first zeolite cages (signal characteristic of EMT structure around 145 ppm) as early as for 4 h of hydrotreatment (see Figure). The signals, at lower chemical shifts, are due to Xe atoms interacting with the amorphous phase which has a more or less structured mesoporosity and differ drastically from one sample to another. Since their position may result from an exchange between various environments and the gas phase, one cannot derive precise information from this part of the spectra because it depends on many parameters including the

morphology of the voids, their relative amount, their connectivity and the degree of polarization of the Xe nuclei. Nevertheless, the presence of a narrow and intense signal (at 90 ppm) observed in the fully-amorphous sample reveals the existence of well-defined meso-voids in the initial gel. Using the relationship established for silica gels by Terskikh *et al.* [2], the average size of those pores can be estimated to be ca. 5.3 nm from the chemical shift value measured at 293 K. This size is in good agreement with the observation of TEM images.



Spectra recorded at 193 K for various synthesis times.

The “EMT” signal is highlighted with a square.

All the results give a very comprehensive analysis of the evolution of the gel morphology, showing in particular the importance of the shell of gel particles in zeolite nucleation, and can be used to control the nucleation in zeolite yielding systems.

#### References:

- [1] C. Martinez, A. Corma, *Coordination Chem. Rev.* **255** (2011) 1558
- [2] V. V. Terskikh, I. L. Moudrakovski, S. R. Breeze, S. Lang, C. I. Ratcliffe, J. A. Ripmeester, A. Sayari, *Langmuir* **18** (2002) 5653

## Talk 26

### Can xenon see the paranematic phase of liquid crystal confined to nanocavities?

A.M. Kantola,<sup>1</sup> J. Karjalainen,<sup>1</sup> S. Komulainen,<sup>1</sup> J. Vaara,<sup>1</sup> J. Lounila,<sup>1</sup> M. Straka,<sup>2</sup> P. Lantto,<sup>1</sup> and V.-V. Telkki<sup>1</sup>

<sup>1</sup> NMR Research Group, University of Oulu, P.O.Box 3000, FIN-90014 Oulu, Finland

<sup>2</sup> Institute of Organic Chemistry and Biochemistry, Academy of Sciences of the Czech Republic, Flemingovo n. 2., 16610 Prague, Czech Republic

Interactions between a liquid crystal molecule and a solid substrate are an important topic in the physics of interfacial phenomena as well as in the applications of electro-optic devices. NMR of dissolved atoms and molecules has successfully been used to obtain information about the properties of variety of materials, including liquid crystals, and the large and extremely polarizable electron cloud of xenon makes it an especially sensitive probe for materials research. NMR spectra of xenon dissolved in liquid crystal can reveal information on the phase transitions and the orientational order as well as the structures of the liquid crystalline phases.

In a recently published theoretical study the orientational order of liquid crystals confined into cylindrical cavities of different sizes was studied with molecular dynamics simulations [1] and the results were later combined with electronic structure calculations on the nuclear shielding of xenon gas dissolved into the same systems [2]. The simulations gave information on how the temperature dependence of the phase structure of the liquid crystal is reflected by the xenon nuclear shielding parameters. The theoretical works also predicted cavity-size-dependent paranematic behaviour in the average ordering related to the interplay of the wall-induced orientational order and the self-organization of the liquid crystal. This paranematic phase is observed above the bulk nematic-isotropic transition temperature and leads to a smooth phase transition instead of a sharp change from an ordered to a disordered phase. To test the theoretical predictions for the xenon nuclear shielding parameters we have carried out experiments on xenon-129 dissolved in liquid crystal Phase 4 confined to cylindrical cavities of



two different sizes [3]. As model systems of cavities we have used aluminum oxide membrane (Anopore™) with cavity diameter of 20 nm as well as mesoporous silica particles (SBA-15) with cavity diameter of 7 nm. The isotropy and the anisotropy of the nuclear shielding tensor of xenon were studied as a function of temperature and the experimental results are compared to the results obtained with the calculations.

**References:**

- [1] J. Karjalainen, J. Lintuvuori, V.-V. Telkki, P. Lantto, J. Vaara, *Phys Chem Chem Phys* **15** (2013) 14047
- [2] J. Karjalainen, J. Vaara, M. Straka, P. Lantto, *Phys Chem Chem Phys* **17** (2015) 7158
- [3] A.M. Kantola, S. Komulainen, J. Lounila, V.-V. Telkki, *manuscript in preparation*

## Talk 27

# EHQE Nuclear Magnetic Resonance Meets Hyperpolarized Gases

M. Sufke<sup>1</sup>, A. Liebisch<sup>2</sup>, B. Blümich<sup>2</sup> and S. Appelt<sup>2,3</sup>

<sup>1</sup>Institute of Energy and Climate Research – Fundamental Electrochemistry (IEK-9),

Forschungszentrum Jülich GmbH, D-52425 Jülich, Germany.

<sup>2</sup>Institut für Technische Chemie und Makromolekulare Chemie (ITMC), RWTH Aachen University, D-52056 Aachen, Germany.

<sup>3</sup>Central Institute for Engineering, Electronics and Analytics – Electronic Systems (ZEA-2), Forschungszentrum Jülich GmbH, D-52425 Jülich, Germany

In my lecture I will present a new technique for sensitive detection of NMR signals, which is based on the coupling between an input coil and an external resonator with a very high quality-factor. This so called External High Quality-Factor Enhanced (EHQE) NMR technique operates best at frequencies ranging from 1 kHz – 10 MHz and has several striking features, such as a very high signal-to-noise ratio that is weakly dependent on the detection frequency and a large flexibility with respect to the size and shape of the sample. EHQE NMR combined with the enhanced magnetization provided by hyperpolarized <sup>129</sup>Xe or by molecules hyperpolarized with Para Hydrogen (PHIP), opens up a large number of applications for compact NMR sensors at low frequencies. I will discuss the basic theory of EHQE-NMR and present a few examples, which show the range of possible applications. This includes microcoil based NMR of  $\mu$ L sized samples at 500 kHz and the detection of rare spins such as <sup>6</sup>Li-ions in small quantities. Finally NMR signals at 166 kHz of hyperpolarized <sup>129</sup>Xe exposed to normal atmospheric conditions can be detected on a surface, allowing online monitoring of the physical and chemical properties of a thin liquid layer.

### References:

- [1] M. Sufke, A. Liebisch, B. Blümich, and S. Appelt, submitted to Nat. Phys.
- [2] J. Colell, P. Türschmann, S. Glöggler, P. Schleker, T. Theis, M. Ledbetter, D. Budker, A. Pines, B. Blümich, and S. Appelt, Phys. Rev. Lett. **110**, 137602 (2013).

**Notes:**

## Talk 28

### Kinetics of Cryptophane-Xenon Complex Formation

Sergey Korchak<sup>1</sup>, Wolfgang Kilian<sup>1</sup>, Lorenz Mitschang<sup>1</sup>

<sup>1</sup> Physikalisch-Technische Bundesanstalt, Abbestr. 2–12, 10587 Berlin

The complex formation of cryptophane-A (CrA) and xenon has been quite extensively studied as a model for host-guest systems governed by van der Waals forces as well as for its importance for magnetic resonance. The reversible binding of xenon to CrA in the mode of slow exchange on the NMR-timescale is pivotal for biomedical applications as individual signals can be assigned in targeting events and sensitivity enhancement through HyperCEST may be employed. The details of host-guest kinetics, however, were barely explored in the past because of a lack of knowledge about the nature of the exchange mechanisms involved and of a lack of suitable experimental approaches for their discovery and quantification. A simple dissociative process where xenon enters an empty CrA or leaves one behind is usually assumed; but little or no attention is paid to degenerate exchange where bound and unbound xenon interchange their binding status directly without a detour of emptying CrA first despite early evidence for such a process found in organic solvents [1]. We thus set out to clarify and quantify the exchange kinetics in CrA-xenon host-guest systems, particularly in aqueous solution.

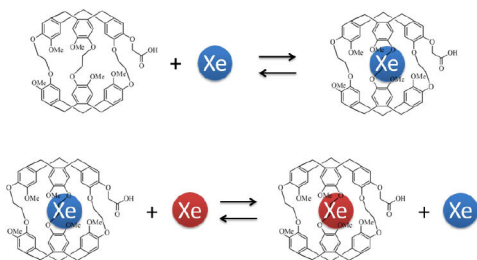


*Fig. 1: dissociative (top) and degenerate (bottom) exchange processes for xenon binding to monoacidic acid CrA.*

Degenerate exchange is not easy to identify. Because that mechanism does not exert an additional change in the position or intensity to the signals assigned to the pools of free and CrA-bound xenon, a discrimination from the dissociative mechanism by hand of a NMR spectrum is not possible. However, both exchange processes are different in their dependence on the amount of free xenon participating in the binding reactions. Thus, we applied saturation- and magnetization-transfer experiments in conjunction with xenon concentration variation to disentangle the exchange network. For example, by saturation transfer from free to CrA-bound xenon pools the complex was found to decay at a rate linearly dependent on the concentration of free xenon only if the degenerate exchange is present while the rate remains constant if solely the dissociative process prevails. In this way, the existence of a degenerate exchange mechanism besides a dissociative process was proven for the first time in aqueous solution, using monoacidic acid CrA and hyperpolarized  $^{129}\text{Xe}$  dissolved in pure water (Fig. 1) [2]. Rate constants of  $19 \pm 1 \text{ s}^{-1}$  and  $5600 \pm 800 \text{ M}^{-1}\text{s}^{-1}$  for dissociative and degenerate exchange, respectively, at 298 K were found.

Experimental schemes were developed and applied in various phases, e. g. aqueous solutions and lipids, for the analysis of the reversible binding of xenon to CrA and for quantification of exchange rates. Knowledge of the details of the exchange kinetics is fundamental to a thorough understanding of the host-guest interaction as well as performance and analysis of experimentation in the various applications.

#### References:

- [1] K. Bartik, M. Luhmer, J.-P. Dutasta, A. Collet, J. Reisse, *J. Am. Chem. Soc.* **120** (1998), 784.
- [2] S. Korchak, W. Kilian, L. Mitschang, *Chem. Comm.* **51** (2015), 1721.

## Talk 29

### Selective Host-Guest Interactions in Metal-Organic Frameworks

**T. W. Kemnitzer,<sup>1</sup> C. Tschense,<sup>1</sup> J. Wack,<sup>1</sup> Y. A. Avadhut,<sup>1</sup> C. D. Keenan,<sup>2</sup> T. Wittmann,<sup>1</sup> K. Bärwinkel,<sup>1</sup> N. Stock,<sup>3</sup> J. Senker<sup>1</sup>**

<sup>1</sup> Inorganic Chemistry III, University of Bayreuth, Universitätsstr. 30, 95447 Bayreuth, Germany

<sup>2</sup> Chemistry Department, Carson-Newman University, Jefferson City, Tennessee 37830, USA

<sup>3</sup> Inorganic Chemistry, University of Kiel, Max-Eyth-Straße 2, 24118 Kiel, Germany

Porous materials offer potential for applications like drug delivery, gas storage and separation as well as sensor design. In particular, within the context of current efforts for the realization of a sustainable energy future, porous materials are of relevance. Most applications rely crucially on the interactions between the framework and the incorporated guests. The lecture will provide an overview of our recent results about introducing and analyzing selective host-guest interactions in series of functionalized metal-organic frameworks based on MIL-53 and MIL-101 topologies. By using postsynthetic modification (PSM) strategies, we aim at introducing supramolecular principles like the lock-key concept based on amino, amide and urea functionalities, respectively [1,2].

Using xenon, carbon dioxide and acetone as local probes we have been able to study the porosity and inter-pore connectivities, the structural and dynamical disorder of anchor groups and guest molecules as well as preferred binding sites. This requires an integral approach combining different techniques like powder X-ray diffraction, sorption measurements, solid-state NMR spectroscopy and computational chemistry. We make use of techniques to hyperpolarize <sup>129</sup>Xe gas to speed up the NMR experiments and apply modern multinuclear and multidimensional NMR techniques to unravel homo- and heteronuclear connectivities and distances. In this way we could follow the reversible breathing mode of MIL53 as a function of temperature and Xe partial pressure (Fig. 1a), which includes a volume change of about 30 %. The adsorption of carbon

dioxide and acetone in MIL-53-X with X= NH<sub>2</sub> and NHCHO was shown to be correlated to strong preferred alignments of the anchor groups based on Rietveld refinements, <sup>13</sup>C-<sup>13</sup>C spin-diffusion and double-quantum correlation experiments (Fig. 1b). Finally, based on a combination of 1D <sup>129</sup>Xe and 2D <sup>1</sup>H-<sup>27</sup>Al HETCOR spectra (Fig. 1c) we investigated the mechanism for the remarkable stabilization of MIL-101 upon PSM with phenyl isocyanate.

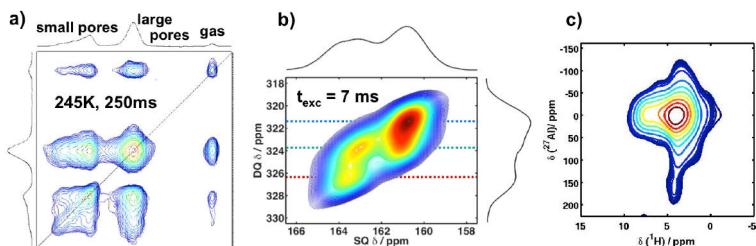


**Fig. 1:** a) <sup>129</sup>Xe EXSY spectrum of MIL-53; b) <sup>13</sup>C-<sup>13</sup>C DQ spectrum of MIL-53-NHCHO; c) <sup>1</sup>H-<sup>27</sup>Al HETCOR spectrum of MIL-101-NHCONH-Ph.

### References:

- [1] J. Wack, R. Siegel, T. Ahnfeldt, N. Stock, L. Mafra, J. Senker, *J. Phys. Chem. C* **117** (2013), 19991.
- [2] T. Wittmann, R. Siegel, N. Reimer, W. Milius, N. Stock, J. Senker, *Chem. Eur. J.* **21** (2015), 314.

## Poster 1

# Monitoring of the structural transition in the highly flexible “gate pressure” Metal-Organic Framework Ni<sub>2</sub>(2,6-ndc)<sub>2</sub>dabco using High-Pressure *in situ* <sup>129</sup>Xe NMR Spectroscopy

**Volodymyr Bon<sup>3</sup>, Herbert C. Hoffmann<sup>1</sup>, Bassem Assfour<sup>2</sup>,  
Fanny Epperlein<sup>1</sup>, Nicole Klein<sup>3</sup>, Silvia Paasch<sup>1</sup>, Irena  
Senkovska<sup>3</sup>, Stefan Kaskel<sup>3</sup>, Gotthard Seifert<sup>2</sup>, Eike Brunner<sup>1</sup>**

<sup>1</sup> Bioanalytische Chemie, <sup>2</sup> Physikalische Chemie, <sup>3</sup> Anorganische Chemie I, Technische Universität Dresden, Fachrichtung Chemie und Lebensmittelchemie, 01062 Dresden, Germany

Metal-Organic Frameworks (MOFs) are crystalline porous materials that comprise of metal ions or clusters that are interconnected by organic ligands forming 3D frameworks with various topologies.[1] The ultra-high surface area, pore volume, precise pore aperture design as well as functionalization potential make these materials especially attractive for gas storage, gas separation, catalysis, sensor technology etc.[2] Among a plethora of MOFs synthesized up to now, there are several dozens of materials that show a unique phenomena of stimuli responsible structural transformation.[3] This phenomenon could be studied in details using combined *in situ* techniques.

In this contribution, we show how the flexible behavior of “gate pressure” MOF Ni<sub>2</sub>(2,6-ndc)<sub>2</sub>dabco, further denoted as DUT-8(Ni) (DUT – Dresden University of Technology) during the Xe adsorption can be understood by the means of *in situ* <sup>129</sup>Xe NMR.[4] The measurements were carried out at 237K using a new, home-made sapphire sample cell allowing sample pressurization directly inside the NMR magnet. The measurements show that only sharp signal of gaseous <sup>129</sup>Xe could be observed in the pressure range 0-12 bar that lies below the gate opening pressure (Fig. 1). Further increasing of the Xe pressure leads to the structural transformation of the material from close to open form. This is accompanied with the appearance of the new broad signal in the <sup>129</sup>Xe NMR spectra at 230 ppm that is referred to the xenon adsorbed in the pores of the MOF. Increasing of the xenon pressure to 18.9 bar (nearby the condensation point of the gas) leads to the appearance of the new peak at 203 ppm in the



$^{129}\text{Xe}$  NMR spectrum that can be interpreted as a signal of condensed xenon.

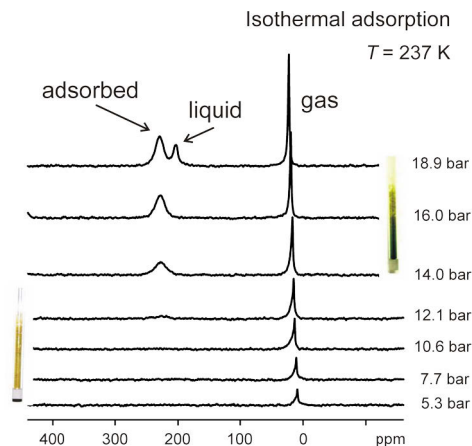


Figure 1.  $^{129}\text{Xe}$  NMR spectra, measured *in situ* during the adsorption of the xenon at 237K.

The desorption of the xenon shows behaviour characteristic for “gate pressure” MOFs. Because “gate closing” pressure is lower than “gate opening” pressure, the signal of adsorbed xenon is present in the  $^{129}\text{Xe}$  NMR spectrum even at the pressure of 1 bar. Using the experimental data, obtained during *in situ* experiment, the preferred adsorption sites and interaction energies of xenon atoms in the open DUT-8(Ni) could also be determined by MD simulations using the DFT-vdW method.[5]

#### References:

- [1] D. J. Tranchemontagne, J. L. Mendoza-Cortés, M. O’Keeffe, O. M. Yaghi *Chem. Soc. Rev.* **38** (2009) 1257-1283.
- [2] Special issue MOFs. *Chem. Soc. Rev.* **43** (2014).
- [3] S. Horike, S. Shimomura and S. Kitagawa, *Nature Chem.* **1** (2009) 695-704.
- [4] N. Klein, C. Herzog, M. Sabo, I. Senkowska, J. Getzschmann, S. Paasch, M.R. Lohe, E. Brunner and S. Kaskel, *Phys. Chem. Chem. Phys.* **12** (2010) 11778-11784.
- [4] H. C. Hoffmann, B. Assfour, F. Epperlein, N. Klein, S. Paasch, I. Senkowska, S. Kaskel, G. Seifert and E. Brunner, *J. Amer. Chem. Soc.* **133** (2011) 8681-8690.

## Poster 2

### ***In-situ* Probing of Catalytic Reaction Dynamics by Means of Xe-129 NMR Spectroscopy**

**M. Dvoyashkin,<sup>1</sup> A. Zaheer,<sup>1</sup> J. Zill,<sup>2</sup> J. Matysik,<sup>2</sup> C. Küster,<sup>1</sup> D. Enke,<sup>1</sup> R. Gläser<sup>1</sup>**

<sup>1</sup> Institute of Chemical Technology, Universität Leipzig, 04103 Leipzig, Germany

<sup>2</sup> Institute of Analytical Chemistry, Universität Leipzig, 04103 Leipzig, Germany

The determination of reaction rates in chemical conversions relies on analysis of the reactant amounts most commonly by *ex-situ* techniques such as chromatography. When these are applied for studying reaction dynamics within nanoporous catalyst, separation of the reaction dynamics from the mass transfer dynamics becomes challenging. In contrast, NMR can be exploited as a non-invasive technique for the *in-situ* detection of the bulk fluids and fluids adsorbed (and reacting) inside the catalyst pores [1].

In this contribution, we demonstrate an approach for an *in-situ* probing of reaction dynamics in Xe-pressurized liquid mixtures by means of Xe-129 NMR spectroscopy. As an example, we focus on the base catalyzed transesterification of sunflower oil with methanol into biodiesel and glycerol. Two peaks corresponding to Xe dissolved in oil and methanol separated by ~50 ppm can be seen on Fig.1 (left, upper spectrum). As the reaction proceeds, a change of the Xe-129 chemical shifts by >20 ppm is observed, which results from the mixing of the initially macroscopically separated liquid components. Two possible scenarios of mixing based on the two-site exchange model and different spatial distribution of liquid domains have been considered for a quantitative description of the observed spectra. For comparison, C-13 NMR data obtained on the identical liquid mixture reveal a maximum change of the signals of the carbon atoms bonded with two oxygen atoms of ~10 ppm (shown by arrows in Fig. 1, right).

The potential of this approach for monitoring reaction dynamics of liquid mixtures inside nanoporous materials will be demonstrated using a controlled pore glass (CPG) with a mean pore width of 5 nm.

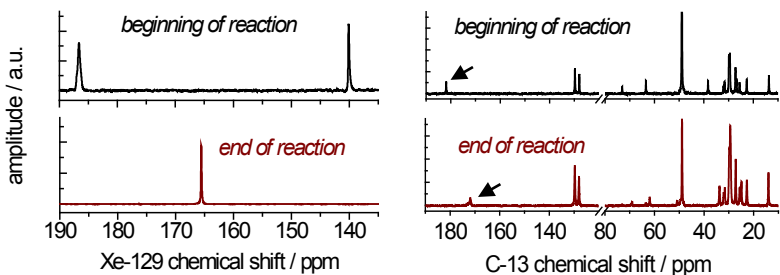


Figure 1: Xe-129 (left) and C-13 (right) NMR spectra of Xe-pressurized sunflower oil/methanol liquid mixture undergoing a transesterification reaction at room temperature into biodiesel and glycerol at the beginning (upper spectra) and at the end of the experiment (bottom spectra) in the presence of potassium hydroxide as a catalyst.

#### References:

- [1] W.P. Zhang, S.T. Xu, X.W. Han, X.H. Bao, *Chem. Soc. Rev.*, **41** (2012) 192-210.

## Poster 3

### **$^{129}\text{Xe}$ NMR of the Xe in Polyimides with Different Glassy States**

**M. Fujita<sup>1</sup> and H. Yoshimizu<sup>1</sup>**

<sup>1</sup>Graduate School of Engineering, Nagoya Institute of Technology, Gokisocho, Showa-ku, Nagoya, 466-8555, Japan. E-mail: yoshimizu.hiroaki@nitech.ac.jp

In general, gas sorption of glassy polymers can be explained by the dual-mode sorption model [1, 2]. This model says the total sorption amounts are consisted with the amounts of Henry and Langmuir type sorption sites. It can be said that the saturation constant in the Langmuir sorption mode corresponds to the unrelaxed volume (so-called "excess free volume") of glassy polymer. The presence of unrelaxed volume in glassy polymers plays an important role in the gas sorption properties as microvoids. Thus, it is possible to understand the behaviors of unrelaxed volume by examining the Langmuir sorption parameters. In this study, polyimide (PI) which is one of glassy polymers was used to clarify the glassy state through the relationships between the microvoids and Xe sorption properties. PI membranes with different glassy states were prepared by CO<sub>2</sub> conditioning. This conditioning was performed as follows; an as-received PI film was put into a stainless chamber, and then CO<sub>2</sub> was introduced to the chamber until a pressure of 60 atm at 25 °C for 20 hrs. After this period, CO<sub>2</sub> was released quickly. Density and Xe sorption amounts of the CO<sub>2</sub>-conditioned PI film was lower and larger than those of as-received PI film, respectively. Xe sorption isotherms of these PI films could be explained successfully on the basis of the dual-mode sorption model.  $^{129}\text{Xe}$  NMR chemical shift of the Xe in PI films downfield shift non-linearly with increasing pressure of Xe. By our proposed analyzing method using the pressure-dependence chemical shifts data and the dual-sorption parameters [3, 4], the mean sizes of the microvoids of PI films could be determined. The size of the microvoids in the CO<sub>2</sub>-conditioned PI film was larger than that of as-received PI film. It was concluded that the microvoids of PI can be some extent controlled by CO<sub>2</sub> conditioning.

## References:

- [1] D. R. Paul, W. J. Koros, *J. Polym. Sci. Polym. Phys. Ed.* **14** (1976) 675.
- [2] H. Hachisuka, Y. Tsujita, A. Takizawa, T. Kinoshita, *Polymer* **29** (1988) 2050.
- [3] T. Suzuki, M. Miyauchi, M. Takekawa, H. Yoshimizu, Y. Tsujita, T. Kinoshita, *Macromolecules* **34** (2001) 3805.
- [4] H. Yoshimizu, *NMR Spectroscopy of Polymers: Innovative Strategies for Complex Macromolecules*; ACS Symposium Series **1077** (2011) 509.

## Poster 4

### Characterisation of Acinar Airspace Involvement in Asthma using Inert Gas Washout and Hyperpolarised <sup>3</sup>Helium Magnetic Resonance

S. Gonem<sup>1</sup>, S. Hardy<sup>2</sup>, N. Buhl<sup>2</sup>, R. Hartley<sup>1</sup>, M. Soares<sup>1</sup>, R. Kay<sup>3</sup>,  
R. Costanza<sup>4</sup>, P. Gustafsson<sup>5</sup>, C.E. Brightling<sup>1</sup>, J. Owers-Bradley<sup>2</sup>, S. Siddiqui<sup>1</sup>

<sup>1</sup> Institute for Lung Health, Department of Infection, Immunity and Inflammation, University of Leicester, United Kingdom

<sup>2</sup> Department of Physics and Astronomy, University of Nottingham, United Kingdom

<sup>3</sup> Novartis Pharmaceuticals, Basel, Switzerland

<sup>4</sup> Chiesi UK Ltd., Cheadle, United Kingdom

<sup>5</sup> Department of Paediatrics, Central Hospital, Skövde, Sweden

This poster is a presentation of work to be published in Journal of Allergy and Clinical Immunology [1].

#### **Background**

The multiple breath washout (MBW) parameter S<sub>acin</sub> is thought to be a marker of acinar airway involvement, but has not been validated using quantitative imaging techniques in asthma.

#### **Objective**

We aimed to utilise <sup>3</sup>He diffusion magnetic resonance (<sup>3</sup>He-MR) at multiple diffusion timescales and quantitative computed tomography (CT) densitometry to determine the nature of acinar airway involvement in asthma.

#### **Methods**

Thirty-seven patients with asthma and seventeen age-matched healthy controls underwent spirometry, body plethysmography, MBW (using the tracer gas sulphur hexafluoride) and He-MR. A subset of patients with asthma (n = 27) underwent quantitative CT densitometry.

#### **Results**

Ninety-four percent (16/17) of patients with an elevated S<sub>acin</sub> had GINA treatment step 4/5 asthma and 13/17 had refractory disease. The apparent diffusion coefficient (ADC) of <sup>3</sup>He at 1s was significantly higher in patients with S<sub>acin</sub>-high asthma compared to healthy controls 0.024 vs 0.017, p < 0.05). S<sub>acin</sub> correlated strongly

with ADC at 1s ( $R = 0.65$ ,  $p < 0.001$ ), but weakly with ADC at 13ms ( $R = 0.38$ ,  $p < 0.05$ ). ADC at both 13ms and 1s correlated strongly with the mean lung density expiratory/inspiratory ratio, a CT marker of expiratory air trapping ( $R = 0.77$ ,  $p < 0.0001$  for ADC at 13ms;  $R = 0.72$ ,  $p < 0.001$  for ADC at 1s).

### **Conclusion**

$S_{acin}$  is associated with alterations in long-range diffusion within the acinar airways and gas trapping. The precise anatomical nature and mechanistic role in severe asthma requires further evaluation.

### **Funding**

This work was funded by the National Institute for Health Research (NIHR), and partly funded through research collaborations with Chiesi Farmaceutici S.P.A. and Novartis Pharmaceuticals and Engineering and Physical Sciences Research Council. Additional funding was received from the Airway Disease Predicting Outcomes through Patient Specific Computational Modelling (funded through an FP7 European Union grant).

### **References:**

- [1] S. Gonem, S. Hardy, N. Buhl, et al., *J.A.C.I.* – to be published (2015), DOI: <http://dx.doi.org/10.1016/j.jaci.2015.06.027>

## Poster 5

### Probing structure and dynamics of silica based materials by continuous-flow hyperpolarized $^{129}\text{Xe}$ -NMR

J. Hollenbach<sup>1</sup>, C. Küster<sup>2</sup>, R. Vialiullin<sup>3</sup>, D. Enke<sup>2</sup>, J. Matysik<sup>\*, 1</sup>

<sup>1</sup> Institut für Analytische Chemie, Universität Leipzig, Linnéstr. 3, 04104 Leipzig, Germany

<sup>2</sup> Institut für Technische Chemie, Universität Leipzig, Linnéstr. 3, 04104 Leipzig, Germany

<sup>3</sup> Abteilung Grenzflächenphysik, Universität Leipzig, Linnéstr. 5, 04103 Leipzig, Germany

\* E-mail: julia.hollenbach@uni-leipzig.de, joerg.matysik@uni-leipzig.de

Silica-based materials such as CPG (Controlled Porous Glasses) and MCM (Mobil Composition of Matter) materials can be synthesized with various textural properties, whereby geometry and pore structure can be modelled well-defined. This makes them attractive construction materials in biotechnology, micro-reaction engineering and heterogeneous catalysis [1].

Hyperpolarized- $^{129}\text{Xe}$ -NMR (HP- $^{129}\text{Xe}$ -NMR) has developed into a well-known tool to characterize porous materials and surfaces. Compared to other surface characterization techniques, such as  $\text{N}_2$ -adsorption and Hg-intrusion, it both provides information about the pore structure and geometry and can be used to probe the interconnectivity of the voids [2,3].

Here we present the application of continuous-flow HP- $^{129}\text{Xe}$ -NMR to study pore properties of CPG samples and the transformation of those glasses into MCM materials. Furthermore, first results to probe the dynamics with selective 1D-EXSY experiments are shown.

#### References:

- [1] D. Enke, F. Janowski, W. Schwieger, *Microporous Mesoporous Mater.* **60** (2003), 19–30.
- [2] I. Moudrakovski, V. Terskikh, C. Ratcliffe, J. Ripmeester, L. Wang, Y. Shin, *J. Phys. Chem. B* **106** (2002), 5938–5946.
- [3] L. Wang, D. Wang, J. Liu, G. Exarhos, S. Pawsey, I. Moudrakovski, *J. Phys. Chem. C* **113** (2009), 6577–6583.



**Notes:**

## Poster 6

### **$^{129}\text{Xe}$ Hyper-CEST for sensing Supramolecular Complexes**

**Jabadurai Jayapaul<sup>1</sup>, Leif Schröder<sup>1</sup>**

<sup>1</sup> ERC project (BiosensorImaging), Leibniz Institut für Molekulare Pharmakologie (FMP), 13125 Berlin, Germany

Supramolecular self-assembly of hosts with guest molecules led to nanofabrication of vehicles and stimuli-responsive materials beneficial for various biomedical applications (e.g., drug delivery & molecular switches)<sup>[1]</sup>. Often, such host-guest interactions are studied using <sup>1</sup>H-NMR at millimolar regime. In the case of cooperative self-assembly occurring between two hosts a molecular thread is required to form ternary complexes<sup>[2]</sup>. Conversely, we have studied such systems with saturation transfer of temporarily bound <sup>129</sup>Xe (Hyper-CEST technique) by relying on the intrinsic molecular motifs of a host for complexing its counterpart.

In this study, for the first time we have investigated the molecular recognition of cucurbit[6]uril (CB6) acting both as a Xe-host and as a host for sulfobutylether (SBE) side chains of anionic  $\beta$ -cyclodextrin ( $\beta$ -CD) host (Captisol®, CS) at low concentrations. Also, we have tried to solubilize higher CB6 payload in water by CS without using any alkaline salts. To begin with, the impact of increasing the concentration of CS with different degrees of substitution (DS) i.e. CS DS6 and CS DS4 (20 -1000  $\mu\text{M}$ ) on the Xe@CB6 association when forming ternary complexes was checked by Hyper-CEST. The spontaneous (dis-)assembly of supramolecular complex was investigated by XeNMR at various temperatures (298 – 310 K) and by <sup>1</sup>H-NMR diffusion measurements. The specific molecular recognition of CB6 for SBE chains available on its complexing partner CS was studied by competitively inhibiting the later using structurally similar butylsulfonate (BS) at different concentrations (100 – 1000  $\mu\text{M}$ ).

Using CS DS6 (1000  $\mu\text{M}$ ) we have solubilized 200  $\mu\text{M}$  of CB6 in water without addition of any solubilizing agents (i.e. ca. ten-fold excess or normal solubility). For 100  $\mu\text{M}$  of CS DS6 plus CB6 (5  $\mu\text{M}$ ) the Xe@CB6 signal displayed an intensity reduction and peak shift compared to Xe@CB6 alone. A linear change in Xe@CB6 peak shift was observed with increasing CS DS6 concentration. To achieve similar change in the chemical shift of Xe@CB6 peak a

higher concentrations of CS DS4 are required (Fig. 1). Different degrees of interaction in the ternary complexes are noted due to varied DS available on CS. The ternary complex at different temperature displayed a moderate drop in the Xe@CB6 peak intensity. In line with this, the diffusion constant of ternary complex ( $2.86 \pm 0.03 \times 10^{-10} \text{ m}^2\text{s}^{-1}$ ) indicated a reduction compared to naked CB7 ( $3.21 \pm 0.02 \times 10^{-10} \text{ m}^2\text{s}^{-1}$ ). The specificity of SBE chains on CS DS6 (100  $\mu\text{M}$ ) for CB6 (5  $\mu\text{M}$ ) was proven by inhibiting them using BS (500  $\mu\text{M}$ ). The Xe@CB6 peak of BS-inhibited ternary complexes was observed at -91.09 ppm compared to CB6 plus CS DS6 (-92.67 ppm) and CB6 alone (-95.66 ppm)(Fig. 1).

In summary, the molecular recognition of CB6 for CS under aqueous conditions was successfully studied using  $^{129}\text{Xe}$  HyperCEST. Our investigations reveal that SBE chains on CS are needed for its ternary complexation with CB6. Hence, these model complex systems will be useful in studying multiple interactions occurring in different molecular architectures (e.g. necklaces, machines, and capsules) employed in drug delivery, sensors and nanotechnology applications.

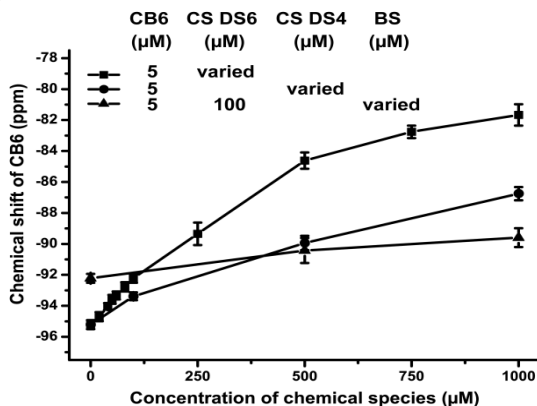


**Figure 1.** Change in  $^{129}\text{Xe}$  chemical shift of Xe@CB6 in ternary complexes at varied DS@CS and BS concentrations. With increasing CS DS6 concentrations the Xe@CB6 peak displays a linear chemical shift changes. Conversely, to observe similar change a higher payload of CS DS4 is required. BS inhibits Xe@CB6 peak in presence of CS DS6 (100  $\mu\text{M}$ ) identical to CS DS4.

## References:

- [1] X. Ma, Y. Zhao, *Chem. Rev.* (2015) DOI: 10.1021/cr500392w.
- [2] M.V. Rekharsky, H. Yamamura, M. Kawai, I. Osaka et. al, *Org. Lett.*, **8** (2006), 815-818.

## Poster 7

### Studying the porosity of MOFs using $^{129}\text{Xe}$ NMR with hyperpolarized Xe

T. W. Kemnitzer,<sup>1</sup> Y. S. Avadhut,<sup>1</sup> E. A. Rössler,<sup>2</sup> J. Senker<sup>1</sup>

<sup>1</sup> Inorganic Chemistry III, University of Bayreuth, Universitätsstr. 30, 95447 Bayreuth, Germany

<sup>2</sup> Experimental Physics II, University of Bayreuth, Universitätsstr. 30, 95447 Bayreuth, Germany

Metal organic frameworks as hybrid materials are showing an increasing relevance in modern applications due to their chemical variability and functionality in combination with high surface areas [1]. Their potential capabilities range from gas separation and storage to catalytic applications. Since pore size and shape is an important property, the study of porosity and adsorption dynamics of these materials has to be examined closely. Using the newly developed design of a two-bodied pumping cell for spin exchange optical pumping, we are able to increase the nuclear spin polarization of  $^{129}\text{Xe}$  by four orders of magnitude while realizing high flow rates. This allows us to detect adsorbed Xenon atoms at low partial pressures and even below the detection limits of conventional gas physisorption [2],[3]. We use this high sensitivity and the  $^{129}\text{Xe}$  chemical shift to probe the porosity of metal organic frameworks (MOFs). For this, we try to correlate observed  $^{129}\text{Xe}$  shifts with pore size distributions determined from Argon physisorption isotherms for several MOFs. The influence of the pore size is studied by changing both the framework and by using isorecticular structures or postsynthetic modification of functional groups (Fig. 1).

In order to determine which properties of the hybrid material cause an influence on the chemical shift we correlate a broad number of MOFs with different framework shapes. Also the effect of electric fields is investigated by comparing MOFs possessing differently charged metal centers. For determination of pore sizes by  $^{129}\text{Xe}$ -NMR the model published from Fraissard [4] is the most prominent one which is working very well for purely inorganic low charged zeolites. However this model does not seem to be valid for MOFs. This could be due to different interactions of the organic linker molecules with adsorbed Xe gas or an electric field caused by the existing metal clusters inside of the network. Both aspects are

completely neglected in the Fraissard model. By combining our results new models to describe pore sizes for materials different to microporous silicates will be developed. Additionally quantum chemical calculations of NMR parameters are used to support our results.

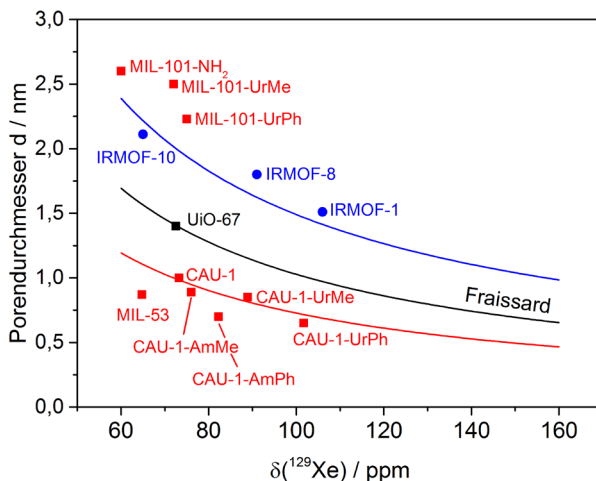


Fig. 1: Correlation of Pore sizes with  $^{129}\text{Xe}$  shifts for different type of MOFs.

#### References:

- [1] G. Férey, *Chem. Soc. Rev.* **37** (2007) **191**.
- [2] P. Ruckdeschel, T. W. Kemnitzer, F. A. Nutz, J. Senker, M. Retsch, *Nanoscale* **7** (2015) **10059**.
- [3] C. D. Keenan, M. M. Herling, R. Siegel, N. Petzold, C. R. Bowers, E. A. Rössler, J. Breu, J. Senker, *Langmuir* **29** (2013) **643**.
- [4] J. Demarquay, J. Fraissard, *Chemical Physics Letters* **136** (1987) **314**.

## Poster 8

### On Dipolar Interaction – From Line Shape to Spin Diffusion to Double Resonance

L. Kraft,<sup>1</sup> A. Potzuweit,<sup>1</sup> A. Schaffner,<sup>1</sup> H.J. Jänsch<sup>1</sup>

<sup>1</sup> Department of Physics, Philipps University Marburg, 35032 Marburg, Germany

Line shape and spin diffusion are fundamental consequences of the dipolar interaction. Both depend strongly and characteristically on the concentration of  $^{129}\text{Xe}$  and on its polarization. Here we present experiments that systematically vary the isotopic content and the polarization of  $^{129}\text{Xe}$  in  $^{132}\text{Xe}$ . The latter being chemically equal but without nuclear spin. Both gases are of 99.9 per cent isotopic quality, so that the  $^{129}\text{Xe}$  concentration could be varied from below 0.01 to nearly 1. For this a mixing system was built allowing the  $^{129}\text{Xe}$  preparation to be the same for all the experiments. A thorough gas phase mixing with the  $^{132}\text{Xe}$  was ensured. The  $\text{N}_2$  buffer gas was separated in a freeze pump cycle. Thus homogeneous Xe films could be deposited onto a metal single crystal surface under ultra high vacuum conditions.

The line shape was measured as a function of polarization and isotopic content. For high concentration and polarization an asymmetric shape was found. Fig 1. shows this. A detailed analysis reveals the third moment of the resonance line to be caused by the B term of the dipole alphabet.

$T_1$  relaxation of Xe films of various thickness and isotopic content were measured and modeled. The metal surface acts as a fast relaxation agent [2] which through spin diffusion leads to the relaxation of the entire film. Diffusion rates in the order of  $1 \dots 9 \cdot 10^{-17} \text{ m}^2/\text{s}$  were found in reasonable agreement with the literature.

Double resonance experiments are under preparation. The idea is to study surface structures such as  $^{13}\text{C}$  graphene on Ir(111). For this  $^{13}\text{C}$  should be polarized through Hartmann-Hahn like spin contact with  $^{129}\text{Xe}$ . Here we want to use a thick polarized xenon film as polarization reservoir that replenishes the contact layer through spin diffusion. The ultra high vacuum NMR probe head should not be altered severely to include the double resonance setup. Therefore a second resonator is coupled to the existing one via cable. Experimental results of the probe behavior are given.

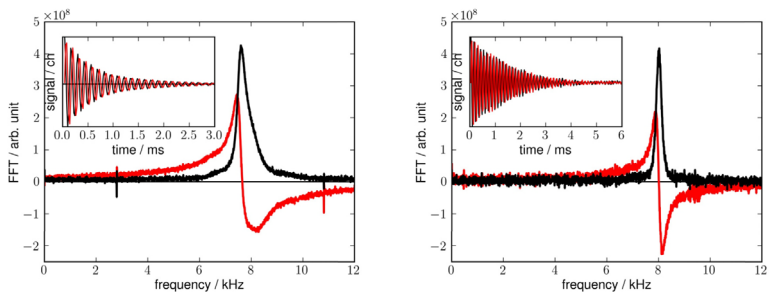


Fig 1. Small angle spectra of  $^{129}\text{Xe}$  at high polarization of pure (left) and 5%(right)  $^{129}\text{Xe}$ . [1]

**References:**

- [1] A. Potzuweit, Dissertation, Marburg 2015.
- [2] H.J.Jansch, P. Gerhard and M. Koch, *PNAS* **101** (2004) 13715.

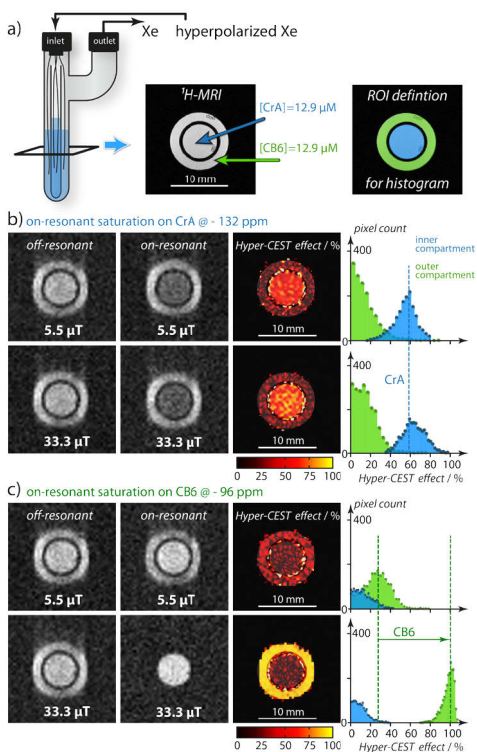
## Poster 9

# Impact of Gas Turnover Rate for Improving Hyper-CEST Sensitivity in Xe Biosensor MRI

M. Kunth,<sup>1</sup> C. Witte,<sup>1</sup> A. Hennig,<sup>2</sup> L. Schröder<sup>1</sup>

<sup>1</sup> ERC Project BiosensorImaging, Leibniz-Institut für Molekulare Pharmakologie (FMP), Robert-Rössle-Straße 10, 13125 Berlin, Germany

<sup>2</sup> Jacobs University Bremen, Department of Life Sciences and Chemistry, Campus Ring 1, 28759 Bremen, Germany



Nuclear magnetic resonance (NMR) signals of the noble gas isotope  $^{129}\text{Xe}$  exhibit outstanding chemical shift sensitivity to its molecular environment. In addition, hyperpolarization of Xe enhances the NMR signal up to 25,000-fold and enable the study of non-covalent Xe interactions with hydrophobic binding sites or hosts. Such molecular hosts can be chemically modified to specifically bind to particular biological targets<sup>[1,2]</sup>. These targeted host, or biosensors, have the potential to facilitate extremely sensitive molecular imaging with MR imaging (MRI) and show utility for early disease detection. By incorporating

the dynamic nature of exchanging Xe and using saturation transfer (Hyper-CEST<sup>[3]</sup>), strikingly low amounts of Xe sensors, down to the picomolar regime, have been detected by both NMR spectroscopy and MR imaging (MRI). Most of these studies used cryptophane-222



(Cr-222 or CrA) as the Xe host. The question of what the lowest detectable host concentration would be, is not trivial to answer as this depends on system parameters such as the saturation pulse and the Xe exchange rate, binding constant and host occupancy. Therefore, knowledge of such parameters is crucial for further biosensor optimization. Conventional quantification methods include direct Xe NMR, isothermal titration calorimetry, etc. that all require large concentrations of the Xe host and, often a different setup. We recently developed a quantitative Hyper-CEST concept<sup>[4]</sup> as a basis for analytical host optimization. Here we demonstrate how the host-intrinsic maximum possible Hyper-CEST effect improves with both the exchange rate and the host occupancy. We exploit this knowledge of a large Xe gas turnover rate and show that the CrA-alternative macrocyclic molecule, cucurbit[6]uril (CB6; also 1:1 Xe complexation, larger exchange rate and larger host occupancy), can (under correct saturation pulse conditions) further amplify the Hyper-CEST sensitivity up to 100-fold<sup>[5]</sup>. Figure 1a) shows the nested NMR tube sample containing equal amounts of CrA and CB6. b-c) off- and on-resonant <sup>129</sup>Xe MRI for low (i.e., 5  $\mu$ T) and high radiofrequency exposure (i.e., 33  $\mu$ T) for CrA and CB6, respectively. Whereas the Hyper-CEST effect (difference of off-resonant minus on-resonant) for CrA does not improve for 33  $\mu$ T, CB6 takes advantage of the stronger saturation field. These results show that a) the gas turnover rate appears to be an appropriate measure for quickly estimating the Hyper-CEST performance of a new Xe-host and b) Hyper-CEST sensitivities could be significantly improved using hosts with larger exchange rates.

#### References:

- [1] P. Berthault, C. Huber, H. Desvaux, *Progr. Nucl. Magn. Reson. Spectros.* **55** (2009) 35-60;
- [2] K.K. Palaniappan, M.B. Francis, A. Pines, D.E. Wemmer, *Isr. J. Chem.* **54** (2014) 104-112;
- [3] L. Schröder, T.J. Lowery, C. Hilty, D.E. Wemmer, A. Pines, *Science* **314** (2006) 446-449;
- [4] M. Kunth, C. Witte, F. Schröder, *J. Chem. Phys.* **51** (2014) 194202;
- [5] M. Kunth, C. Witte, A. Hennig, L. Schröder, *Chem. Sci.* (2015) in press.

## Poster 10

### Clathrate structures discovered by combination of $^{129}\text{Xe}$ NMR spectroscopy with crystal structure predictions

M. Selent,<sup>1,2</sup> J. Nyman,<sup>3</sup> M. Ilczyszyn,<sup>2</sup> P. Bygrave,<sup>3</sup> J. Jokisaari,<sup>1</sup>  
G. M. Day,<sup>3</sup> P. Lantto<sup>1</sup>

<sup>1</sup> NMR Research Group, Faculty of Science, University of Oulu, Finland

<sup>2</sup> Faculty of Chemistry, Wrocław University, Poland

<sup>3</sup> School of Chemistry, University of Southampton, UK

Already the early work of Ripmeester and Davidson [1] of clathrated xenon revealed the potential of  $^{129}\text{Xe}$  NMR in studies of inclusion compounds. While clathrates are fairly easy to produce and measure by  $^{129}\text{Xe}$  NMR, determination of their X-ray crystal structure may sometimes be experimentally challenging. Here we demonstrate that the combination of experimental and computational  $^{129}\text{Xe}$  NMR can be used to distinguish the most probable one from the numerous high-energy porous clathrate structures generated by the crystal structure prediction (CSP) calculations [2].

Unlike *p*-fluorophenol clathrate, crystal structures of *o*- and *m*-fluorophenol xenon clathrates have, to our knowledge, never previously been determined. In this work, we have measured  $^{129}\text{Xe}$  NMR spectra of *o*- and *m*-fluorophenol. As their structures are unknown, we have performed comprehensive and state-of-the-art CSP calculations for them with the specific aim to predict physically realistic xenon clathrate complexes, whose modeled  $^{129}\text{Xe}$  NMR parameters could be compared with measured spectra.

The exceptional sensitivity of the Xe shielding to its environment allows comparisons between observed and calculated isotropic and anisotropic chemical shifts that can be used to directly confirm or reject hypothetical clathrate structures. Based on these comparisons, we propose structures for the two clathrates [3].

#### References:

- [1] J. Ripmeester and D. Davidson, *J. Mol. Struct.* **75**, (1981) 67–72.
- [2] J. T. A. Jones, T. Hasell, X. Wu, J. Bacsá, K. E. Jelfs, M. Schmidtman, S. Y. Chong, D. J. Adams, A. Trewin, F. Schiffman, F. Cora, B. Slater, A. Steiner, G. M. Day and A. I. Cooper, *Nature* (2011), **474**, 367–371
- [3] M. Selent, J. Nyman, M. Ilczyszyn, P. Bygrave, J. Jokisaari, G. M. Day, P. Lantto, *in preparation* (2015).

**Notes:**

## Poster 12

### A doubly responsive probe for the detection of Cys4-tagged proteins

**E. Mari<sup>ad</sup>, N. Kotera<sup>a</sup>, E. Dubost<sup>a</sup>, G. Milanole<sup>a</sup>, E. Doris<sup>a</sup>, E. Gravel<sup>a</sup>, N. Arhel<sup>b</sup>, T. Brotin<sup>c</sup>, J.-P. Dutasta<sup>c</sup>, J. Cochrane<sup>c</sup>, C. Boutin<sup>d</sup>, E. Léonce<sup>d</sup>, P. Berthault<sup>d</sup>, B. Rousseau<sup>a</sup>**

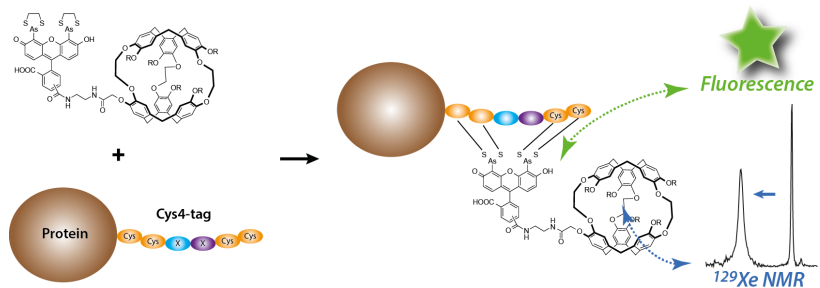
<sup>a</sup> iBiTec-S/SCBM, LabEx LERMIT, CEA Saclay, 91191 Gif-sur-Yvette, France.

<sup>b</sup> Inserm U941, Hôpital St Louis, 1 avenue Claude Vellefaux, 75010 Paris, France

<sup>c</sup> Laboratoire de Chimie, CNRS, Ecole Normale Supérieure de Lyon, 46 Allée d'Italie, 69364 Lyon Cedex 07, France

<sup>d</sup> CEA Saclay, IRAMIS, NIMBE, UMR CEA/CNRS 3685, Laboratoire Structure et Dynamique par Résonance Magnétique, 91191 Gif-sur-Yvette, France

Recombinant proteins bearing a tag are crucial tools for assessing protein location or function. Small tags such as Cys4 tag [1] (tetracysteine; Cys–Cys–X–X–Cys–Cys) are less likely disrupt protein function in the living cell than green fluorescent protein [2]. Herein we report the first example of the design and synthesis of a dual fluorescence and hyperpolarized  $^{129}\text{Xe}$  NMR-based sensor of Cys4-tagged proteins [3]. This sensor becomes fluorescent when bound to such Cys4-tagged peptides, and the  $^{129}\text{Xe}$  NMR spectrum exhibits a specific signal, characteristic of the biosensor-peptide association.



*Principle of action of the biosensor on Cys4-tagged proteins*

## References

- [1] B. A. Griffin. *Science*, **281** (1998) 269-272.
- [2] Roger Y. Tsien. *Ann. Rev. of Biochemistry*, **67** (1998) 509-544.
- [3] N. Kotera et al., *Chem. Comm*; DOI: 10.1039/C5CC04721H.

## Poster 13

### *In situ* $^{129}\text{Xe}$ and $^{13}\text{C}$ NMR spectroscopic investigations of the porosity switching in $\text{Zn}_2(\text{BME-bdc})_x(\text{DB-bdc})_{2-x}\text{dabco}$

J. Pallmann<sup>1</sup>, H. C. Hoffmann<sup>1</sup>, V. Bon<sup>2</sup>, E. Eisbein<sup>3</sup>, I. Schwedler<sup>4</sup>, I. Senkovska<sup>2</sup>, R. Fischer<sup>4</sup>, G. Seifert<sup>3</sup>, S. Kaskel<sup>2</sup>, E. Brunner<sup>1</sup>

<sup>1</sup> Technische Universität, Bioanalytische Chemie, Bergstraße 66, 01062 Dresden, Germany

<sup>2</sup> Technische Universität, Anorganische Chemie, Bergstraße 66, 01062 Dresden, Germany

<sup>3</sup> Technische Universität Dresden, Theoretische Chemie, Bergstraße 66b, 01062 Dresden, Germany

<sup>4</sup> Ruhr-Universität Bochum, Anorganische Chemie II, Universitätsstraße 150, 44801 Bochum, Germany

Xenon is an attractive and frequently used probe atom for NMR spectroscopic investigations due to its high sensitivity for interactions with its environment. Even small changes in the electron environment influence the shielding of the nucleus. Hence, the chemical shift covers a large chemical shift range (up to 7000 ppm).  $^{129}\text{Xe}$  NMR spectroscopy is often used for pore structure characterization of zeolites, porous carbons, microporous polymers and also metal-organic frameworks (MOFs) [1].

$^{13}\text{C}$  NMR spectroscopy of adsorbed  $^{13}\text{CO}_2$  is a complementary method for two reasons:

- (1)  $\text{CO}_2$  is polar in contrast to xenon,
- (2)  $\text{CO}_2$  has a rather insensitive isotropic chemical shift – but a pronounced chemical shift anisotropy (CSA) giving rise to residual CSA in the adsorbed state.

The adsorption of carbon dioxide and xenon by the  $\text{Zn}_2(\text{BME-bdc})_x(\text{DB-bdc})_{2-x}\text{dabco}$  ( $x = 2.0; 1.5; 1.0; 0.5; 0$ ) MOF-series and its “parent MOF”  $\text{Zn}_2(\text{bdc})_2(\text{dabco})$  was studied by *in situ*  $^{13}\text{C}$  and  $^{129}\text{Xe}$  NMR spectroscopy [2]. The modification of the “bdc”-side chains of the parent MOF leads to a flexible MOF-lattice of  $\text{Zn}_2(\text{BME-bdc})_x(\text{DB-}$

bdc)<sub>2</sub>-x-dabco in comparison to the relatively rigid Zn<sub>2</sub>(bdc)<sub>2</sub>(dabco). During adsorption of CO<sub>2</sub>, these flexible materials show a phase transition from a narrow to a large pore state, the so called “breathing” transition accompanied by pronounced CO<sub>2</sub> adsorption. The breathing behavior of the MOF-lattice can be investigated by monitoring the <sup>13</sup>C NMR signal of adsorbed CO<sub>2</sub>. In contrast to CO<sub>2</sub>, the <sup>129</sup>Xe NMR spectra just show weak signals due to minor amounts of adsorbed xenon for the flexible MOFs – although xenon is readily adsorbed by the non-flexible parent compound. This observation implies that the pores of the flexible compounds are hardly accessible for xenon atoms. That means, the flexible compounds are highly selective. Polar gases such as CO<sub>2</sub> induce the breathing transition and are readily adsorbed beyond a certain threshold pressure. In contrast, unpolar gases like xenon atoms hardly penetrate into the pore system and are not able to induce the breathing transition.

#### References:

- [1] H. C. Hoffmann, M. Debowski, P. Müller et al., *Materials* **5** (2012) 2537-2572.
- [2] V. Bon, J. Pallmann, E. Eisbein et al., *Micropor. & Mesopor. Mater.* **216** (2015) 64-74.

bdc = 1,4-benzenedicarboxylate, dabco = 1,4-diazabicyclo[2.2.2]octane, BME-bdc = 2,5-bis(2-methoxyethoxy)-1,4-benzenedicarboxylate, DB-bdc = 2,5-dibutoxy-1,4-benzenedicarboxylate

## Poster 14

### Absolute measurement of the Xe polarization

M. Repetto, P. Blümner, W. Heil, S. Karpuk and S. Zimmer

Johannes Gutenberg University, Staudingerweg 7 55128 Mainz, Germany

The polarization degree of HP Xe ( $P_{Xe}$ ) is usually determined via comparison of the NMR signals obtained from a sample of HP-Xe to one which is thermally polarized (typically  $^1H_2O$  or Xe). The difference between both samples such as pressure, signal intensity and measurement procedure could lead to many experimental uncertainties, which are not easy to estimate [1].

We overcame these experimental difficulties by developing a simple, accurate and inexpensive method to determine  $P_{Xe}$  by directly measuring its macroscopic magnetization in a static magnetic field. This method can determine polarizations over 2 % and it has a sensitivity better than 0.2%bar generating nearly no polarization losses. In addition, this method can be used for all HP gases without further modifications [2].

#### References:

- [1] E. Wilms, M. Ebert, W. Heil, R. Surkau, *Nucl. Ins. and Meth. in Phys Res. A* **401** (1997) 491-498.
- [2] M. Repetto, P. Blümner, W. Heil, Publication in preparation.



**Notes:**

## Poster 15

### Ultra-narrow Line Diode Laser Systems for Optical Pumping of K, Rb, Cs, and Ar Gases

**A. Ryasnyanskiy,<sup>1</sup> L. Chase,<sup>1</sup> T. Wood,<sup>1</sup> V. Smirnov,<sup>1</sup> O. Mokhun,<sup>1</sup> A. Glebov,<sup>1</sup> L. Glebov,<sup>2</sup>**

<sup>1</sup>OptiGrate Corp, 562 S. Econ Cir., Oviedo, Florida 32765, USA

<sup>2</sup>CREOL / The College of Optics and Photonics, University of Central Florida, Orlando, Florida 32816-2700, USA

High power diode lasers with GHz emission bandwidth have a great potential for applications in Spin Exchange Optical Pumping (SEOP), Diode Pumped Alkali vapor (cesium, rubidium, and potassium) Lasers (DPAL), optically pumped rare gas metastable lasers, Raman spectroscopy, and atom cooling. All of these applications require excitation of alkali atoms to upper states by resonant pump light within ultra-narrow resonant transition width.

Laser diode bars (LDBs) can be efficiently used to provide high optical power lasing with the emission bandwidth of several nanometers. The wide band emission of LDBs can be substantially narrowed by using of thick volume Bragg gratings (VBGs) recorded in photo-thermo-refractive (PTR) glass. Precise temperature control of the VBG allows wavelength positioning accuracy better than 1 pm. We present the results of the development of laser diode systems operating at variety of wavelengths and covering different application areas: SEOP (770 nm for K, 794.7 for Rb), DPAL (780 nm – Rb, 852 nm – Cs), Raman spectroscopy (785 nm), and pumping of rare gas (Ar) metastable laser (811 nm). The narrowband emission spectra are presented in the Fig. 1. Depending on the specific application requirements laser linewidths can differ from 15 pm to 100 pm.

The systems produce from 30 to 100 W of circularly polarized or unpolarized light and have a unique capability of tuning both the emitting wavelength in a range of about 300 pm as well as the laser linewidth. The VBG-LDB laser systems can combine several wavelengths (e.g., 795 and 770 nm) with individual control of each wavelength position to match transitions of different gases for Hybrid SEOP applications. Using VBGs for laser resonator longitudinal mode selection allowed us to narrow the linewidth of individual LDBs

down to 15 pm (<10 GHz) with a signal-to-noise ratio exceeding 20 dB.

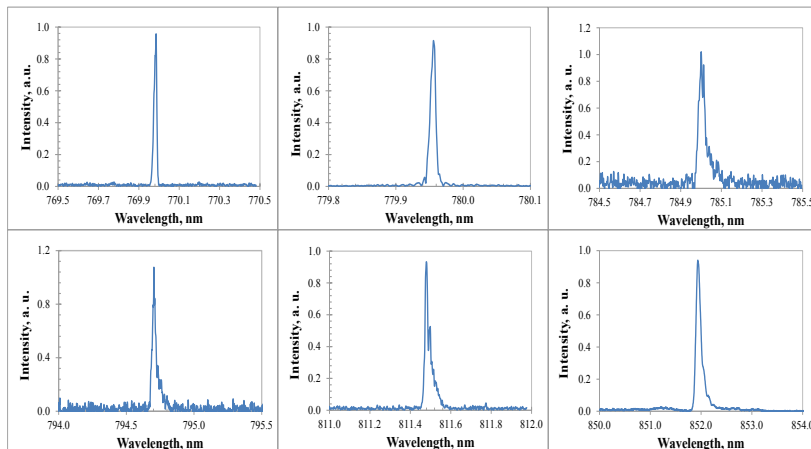


Fig. 1. Narrowband spectra of laser diodes systems operating at various wavelengths.

## Poster 16

### ***In situ* variable pressure $^{129}\text{Xe}$ NMR of zirconium-based metal organic frameworks**

**J. Schaber,<sup>1</sup> I. Senkovska,<sup>2</sup> S. Kaskel<sup>2</sup>, E. Brunner,<sup>1</sup>**

<sup>1</sup> Department of Chemistry and Food Chemistry, Bioanalytical Chemistry, TU Dresden, Bergstrasse 66, D-01062 Dresden, Germany

<sup>2</sup> Department of Chemistry and Food Chemistry, Institute of Inorganic Chemistry, TU Dresden, Bergstrasse 66, D-01062 Dresden, Germany

Metal organic frameworks (MOF) gained increasing research interest during the last years. Zirconium-based MOFs such as UiO-66, UiO-67, and DUT-67 are important with respect to applications due to their high thermostability. All these MOFs contain the same zirconium oxide cluster. However, they differ in porosity because different organic linkers were used for their synthesis. *In situ* variable pressure  $^{129}\text{Xe}$  NMR spectroscopy at pressures up to 20 bar is applied in order to characterize the adsorption/desorption behavior of these MOFs. Due to their similar chemical composition, the pore walls provide a similar chemical environment for adsorbed xenon - but the pore size is different. A correlation between pore size and  $^{129}\text{Xe}$  chemical shift is then observed.

Figure 1 shows the  $^{129}\text{Xe}$  NMR chemical shift for adsorbed xenon on UiO-66, UiO-67 and DUT-67 at 237 K. The isotherms resemble a type I isotherm, based on IUPAC classification. UiO-66 exhibits the smallest pores and therefore highest chemical shifts. It is also remarkable that the chemical shift exceeds that of liquid xenon at 237 K (203 ppm). This is due to the fact that xenon-wall interactions are predominating in micropores even if the pore system is completely filled [1]. UiO-67 and DUT-67 have nearly the same pore sizes and their  $^{129}\text{Xe}$  NMR chemical shifts are consequently similar.

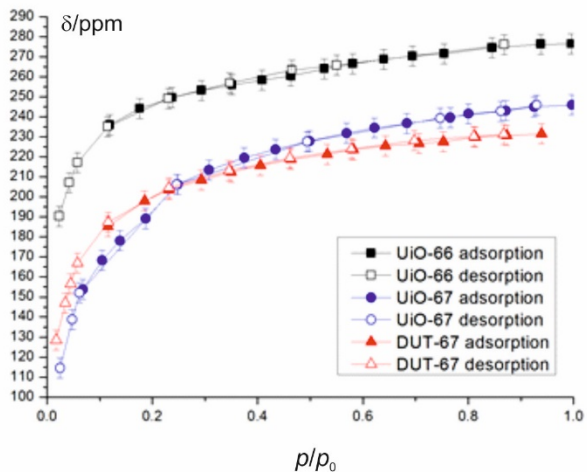


Figure 1:  $^{129}\text{Xe}$  NMR shift of UiO-66(squares), UiO-67(blue circles) and DUT-67(red triangles) at 237 K.

### References:

- [1] M. Oschatz, H.C. Hoffmann, J. Pallmann, J. Schaber, L. Borchardt, W. Nickel, I. Senkovska, S. Rico-Francés, J. Sivestre-Albero, S. Kaskel, E. Brunner, *Chem. Mater.* **2014**, 26, 3280–3288.

## Poster 17

### Using in situ Raman and NMR Spectroscopies to Map the Dependences of Spin-Exchange Optical Pumping and Energy Transport on Xenon Density

J.G. Skinner<sup>1</sup>, H. Newton<sup>1</sup>, J. Birchall<sup>1</sup>, N. Whiting<sup>2</sup>, M. J. Barlow<sup>1</sup>  
& B. M. Goodson<sup>3</sup>

<sup>1</sup> Sir Peter Mansfield Magnetic Resonance Centre, University of Nottingham, NG7 2RD, UK

<sup>2</sup> The University of Texas MD Anderson Cancer Center, Houston, TX 77030, USA

<sup>3</sup> Dept. of Chemistry and Biochemistry, Southern Illinois University, Carbondale, IL 62901, USA

Hyperpolarised xenon (HPXe) has been used to study a number of increasingly diverse applications, including biomedical imaging of the lungs, spectroscopic studies of surfaces and biological systems, and in low-field imaging [1,2]. HPXe is commonly produced by SEOP, and for most applications it is desirable to maximize the resulting polarisation. However, complex in-cell dynamics and acute sensitivity to a number of experimental variables make optimization for polarisation difficult.

In 2001, Walter et al. [3] showed that it is possible to use Raman spectroscopy of N<sub>2</sub> to probe in-cell SEOP temperatures. Members of our research group have since enhanced the sensitivity of this Raman approach [4], reducing acquisition times and thus enabling real-time measurements of elevated internal gas temperatures across the cell—permitting study of how energy is transferred and transported from the laser to the gas, and ultimately to cell walls.

The work presented here exploits these improvements, and combines it with the portability of the Raman probe to obtain rotational N<sub>2</sub> temperature measurements ( $T_{N_2}$ )—and hence, the actual temperatures of the SEOP gas mixtures—at three positions within the OP cell along the pump laser axis during a single SEOP build-up experiment. These measurements, when combined with in situ NMR measurements of <sup>129</sup>Xe polarisation ( $P_{Xe}$ ), provide an insight into dynamics of the in-cell energy transport. Furthermore, the dependence on xenon density ( $[Xe]$ ) is important to study as  $[Xe]$

is expected to affect energy transport during SEOP in two ways: (1) by reducing Rb electron spin polarisation ( $P_{Rb}$ ), and hence increasing laser absorption; and (2) by contributing to a lower thermal conductivity for the gas mixture.

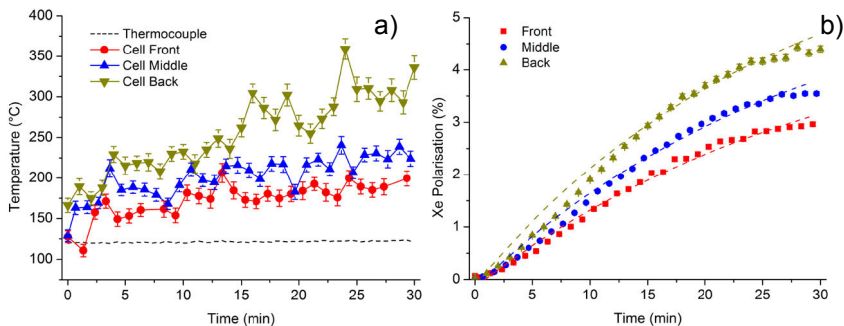


**Fig. 1:** Time and position dependence of  
**(a)** Rotational  $N_2$  temperatures, measured using Raman spectroscopy, and  
**(b)**  $^{129}\text{Xe}$  polarisation, measured using low-field NMR, for a

### References:

- [1] Goodson, B. M., *J. Magn. Reson.* **155** (2002)
- [2] Oros, A. M., Shah N. J., *Phys. Med. Biol.* **49** (2004)
- [3] Walter, D. K., *et al.*, *Phys. Rev. Lett.*, **86** (2001)
- [4] Newton, H., *et al.*, *Appl. Phys. B*, **115** (2013)

## FEM Analysis of Diffusive Exchange of Hyperpolarised $^{129}\text{Xe}$ in the Human Lungs using Realistic Histology-Based Geometries

Neil J Stewart, Juan Parra-Robles, Jim M Wild

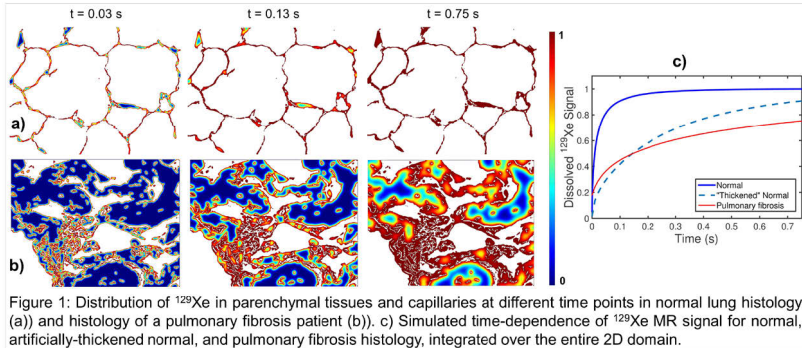
Academic Unit of Radiology, University of Sheffield, Sheffield, United Kingdom

**Introduction:** Chemical shift saturation recovery (CSSR) NMR with hyperpolarised  $^{129}\text{Xe}$  is an effective probe of pulmonary gas-exchange dynamics, enabling quantification of lung microstructural changes via analytical diffusion modelling (e.g., alveolar septal thickening in pulmonary fibrosis [1,2]). However, existing 1D gas-exchange models require physiologically unrealistic assumptions, including homogeneity of septal thickness across the lungs [1,3]. In this work, finite-element (FEM) analysis of xenon diffusive-exchange and blood-flow in the alveoli, lung tissues and capillaries was performed using 3D cylindrical models and realistic alveolar geometries derived from 2D human lung histology.

**Methods:** FEM simulations of xenon diffusive gas-exchange and blood-flow in human lungs were implemented in COMSOL Multiphysics, considering two geometrical situations: i) 3D cylindrical capillaries of uniform thickness with a variable tissue lumen layer; ii) 2D histological sections of human alveoli (from normal lungs and lungs of pulmonary fibrosis patients), segmented and binarised. Interstitial fibrosis was additionally simulated by uniform thickening of the tissues of normal lung sections. Simulations of  $^{129}\text{Xe}$  CSSR NMR experiments were run from time  $t=0$ , to  $t=0.75$  s; time-step=0.001 s.

**Results & Discussion:** Simulated  $^{129}\text{Xe}$  MR signal dynamics from the 3D uniform cylinder models agreed well with previous  $^{129}\text{Xe}$  CSSR data. The lung tissue and capillaries of normal histology sections saturated rapidly (Fig 1) compared with the artificially-thickened tissues, in which there was increased diffusion-limitation of gas-exchange. The  $^{129}\text{Xe}$  magnetisation distribution in histology sections of pulmonary fibrosis was considerably more heterogeneous than in normal samples, altering the shape of the signal dynamics.





To simulate the effect of blood-flow – which causes additional signal in  $^{129}\text{Xe}$  CSSR from xenon distal to the alveoli, preventing an asymptotic steady state of signal at long diffusion times – histology sections were extruded into 3D and “plug” flow was implemented perpendicular to the plane. The addition of this blood-flow induced signal at later diffusion times yielded improved agreement between simulations and previous in-vivo MR data.

**Conclusion:** FEM analysis of  $^{129}\text{Xe}$  diffusive-exchange using realistic histology-based geometries accounts for disease heterogeneity in modelling of  $^{129}\text{Xe}$  MR data, which should lead to more accurate quantification of lung microstructure in fibrotic lung diseases.

**Acknowledgements:** Special thanks to Dr. William Wallace, University of Edinburgh for provision of histology sections.

#### References:

- [1] S. Patz et al., *New J Phys.* **13** (2011).
- [2] N. J. Stewart et al., *Magn Reson Med.* doi:10.1002/mrm.25400 (2014).
- [3] Y. Chang, *Magn Reson Med.* **69** (2013).

## Poster 20

### **MRI of metabolically labeled glycans using Hyper-CEST xenon biosensors in a live-cell bioreactor.**

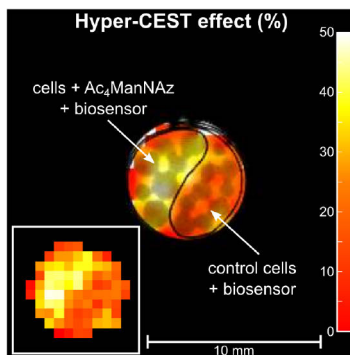
**C. Witte,<sup>1</sup> L. Schröder,<sup>1</sup>**

<sup>1</sup> Leibniz-Institut für Molekulare Pharmakologie (FMP), ERC Project BiosensorImaging, Berlin, Germany.

Hyper-CEST xenon biosensors are a novel class of MRI contrast agents that, using saturation transfer, can achieve very high sensitivity. Recent work demonstrated the first imaging of molecular targets using xenon biosensors *in cellulo*, though the question remains if xenon biosensors can address cellular targets that have proven challenging for proton MRI. An ideal case study to address this question is molecular imaging of metabolically-labeled cell-surface glycans.

Glycosylation is one of the most common post-translational modifications and has many important functions, e.g. altered glycosylation modulates the immune system and is a hallmark of malignancy and carcinogenesis [1]. A popular technique to observe changes to the glycome in living organisms is with fluorescent probes targeted to metabolically labeled glycans via bioorthogonal chemistry. This technique taps into the underlying metabolic processes of the cell to introduce unnatural sugars bearing bioorthogonal functional groups into cellular glycans [2]. Such bioorthogonal functional groups are not naturally present in cells and are biologically inert but will react with other complimentary bioorthogonal functional groups. Conventional paramagnetic MRI contrast agents have been synthesized that aim to utilize this technique [3] but recent attempts have failed to generate sufficient contrast both *in vivo* and *in cellulo* [4].

We synthesized a dual mode fluorescence/xenon MRI contrast agent to target cell surface glycosylation. The biosensor consists of a xenon host (cryptophane-A), fluorescent dye and bioorthogonal cyclononyne derivative attached to a peptidic backbone. Three steps were required to image metabolically labeled glycans using this biosensor. First, cells were incubated with  $\text{Ac}_4\text{ManNAz}$  sugar for three days. Second, they were incubated with the biosensor for 30 min. Control cells were also incubated with the biosensor but did not receive  $\text{Ac}_4\text{ManNAz}$ . Labeling was confirmed using flow cytometry. Cells were



**Hyper-CEST xenon MRI** successfully localizes the labeled cells to the correct compartment. Insert displays the raw Hyper-CEST data.

embedded in alginate with labeled cells placed in one compartment and control cells in another compartment of our custom NMR-compatible live-cell bioreactor. Finally, using Hyper-CEST xenon MRI we successfully localized the labeled cells to the correct compartment (approximate cryptophane-A concentration of 150 nM) demonstrating successful targeted MRI of cell surface glycosylation [5]. Not only does this represent a big step forward for targeted xenon biosensors, but this also further opens up the glycome to investigation via MRI.

#### References:

- [1] Campbell et al., Mol. Biosyst. 2007 3(3):187-94.
- [2] Dube and Bertozzi, Nat. Rev. Drug Discov. 2005 4(6):477-88.
- [3] Lemieux et al., J. Am. Chem. Soc. 1999 121:4278-4279
- [4] Neves et al., Bioconjug. Chem. 2013 24(6):934-41.
- [5] Witte et al., Angew. Chem. 2015 54:2806–2810.

## Poster 21

### Novel high-volume, standard pressure $^{129}\text{Xe}$ SEOP polarizer with spectrally width narrowing laser system

Anna Wojna-Pelczar<sup>1,2</sup>, Tadeusz Pałasz<sup>2</sup>

<sup>1</sup> Central European Institute of Technology (CEITEC), Masaryk University, Kamenice 753/5, 625 Brno, Czech Republic

<sup>2</sup> Smoluchowski Institute of Physics, Jagiellonian University, Lojasiewicza 11, 30348 Krakow, Poland

The introduction of hyperpolarized noble gases  $^3\text{He}$  and  $^{129}\text{Xe}$  delivered a great tool for growing number of applications, ranging from medical imaging [1, 2, 3, 4] to spectroscopy studies. The specific properties of xenon, mostly arising from the large polarizability of its electron cloud and then the chemical shift, makes this noble gas a very interesting NMR probe for biological systems [5] and is commonly used in non-invasive lung diagnosis for MRI applications.

Rising requirements for large volumes of hyperpolarized gases could be realized by efficient polarizers and such as a novel polarizer for  $^{129}\text{Xe}$  presented here. This high-scale production polarizer works based on the Spin Exchange Optical Pumping (SEOP) method. Design of polarizer requires a spectral width narrowing [6] and stabilization of the emission wavelength of multimode high-power laser diode bar.

Three main parts of this polarizer will be presented: the high-power (tens of Watts) laser diode system spectrally narrowed with Volume Bragg Gratings (VGB) for rubidium optical pumping, the high-volume SEOP cell and the cryogenic accumulation system for hyperpolarized  $^{129}\text{Xe}$ . This overview of the motivation and current status of our SEOP polarizer project and research on processes like spin-exchange and relaxation mechanisms are the main topics of this presentation.

#### References:

- [1] M. S. Albert et al *Nature* **370** (1994) 6486, 199
- [2] G. Collier et al *J. Appl. Phys.* **113** (2013) 204905
- [3] G. Norquay et al *J. Appl. Phys.* **113**, (2013) 044908
- [4] F. W. Hersman et al *Acad. Radiol.* **15** (2008) 683
- [5] B. M. Goodson *J. Magn. Reson.* **155** (2002) 157
- [6] B. Chann et al *Optics Letters* **25** (2000) 18

**Notes:**

## Poster 22

# Fine Structure of Glassy State of Polymers through the $^{129}\text{Xe}$ NMR Chemical Shift and Xe Sorption Properties

H. Yoshimizu<sup>1</sup>

<sup>1</sup>Graduate School of Engineering, Nagoya Institute of Technology, Gokiso-cho, Showa-ku, Nagoya, 466-8555, Japan.  
E-mail: yoshimizu.hiroaki@nitech.ac.jp

The gas solubility, diffusivity, and permeability (gas transport properties) of polymer are directly influenced from their structural characteristics. The microvoids exist in glassy polymers are considered to correlate with unrelaxed volume (so-called as "excess free volume"), which are the space remained when polymer becomes glassy state and is regarded as the segmental mobility of main chains are frozen. Evaluation of gas sorption properties for glassy polymers can provide useful information about the microvoids. In this study, the microvoids in glassy polymers were investigated by Xe sorption and  $^{129}\text{Xe}$  NMR measurements including our previous data [1-4]. Fine structures of the glassy polymers are able to image through the analysis of  $^{129}\text{Xe}$  NMR chemical shifts, and the clarification of relationship between gas diffusion properties and the higher-ordered structures are possible. Xe sorption isotherms of glassy polymers have been successfully interpreted by the dual-mode sorption model, so that, the dual-mode sorption parameters were determined by non-linear least square method. The  $^{129}\text{Xe}$  NMR chemical shift of the Xe in the samples showed non-linear low-field shift with increasing sorption amount of Xe, because of fast exchange of Xe atoms between two sites explained by the dual-mode model. From this Xe-density dependence of the  $^{129}\text{Xe}$  NMR chemical shift, it has been able to estimate mean size of the microvoids in glassy polymer. It was found that the mean diameter of the microvoid in polyvinylchloride is very close to van der Waals diameter of Xe atom, and Xe sorption is not detectable for ethylene-vinylalcohol copolymer whose free space size was smaller than Xe atom. From these findings, it is demonstrated that  $^{129}\text{Xe}$  NMR

spectroscopy is a powerful technique to characterize the fine structures of glassy polymers.

**References:**

- [1] T. Suzuki, M. Miyauchi, M. Takekawa, H. Yoshimizu, Y. Tsujita, T. Kinoshita, *Macromolecules* **34** (2001) 3805.
- [2] H. Yoshimizu, *NMR Spectroscopy of Polymers: Innovative Strategies for Complex Macromolecules; ACS Symposium Series* **1077** (2011) 509.
- [3] H. Yoshimizu, S. Ohta, T. Asano, T. Suzuki, Y. Tsujita, *Polymer J.* **44** (2012) 821.
- [4] H. Yoshimizu, T. Murakami, T. Suzuki, Y. Tsujita, *Polymer J.* **44** (2012) 827.

## 4. Sponsors

**Thanks for financial support!**



Gesellschaft von Freunden und  
Förderern der TU Dresden e. V.



